AN ABSTRACT OF THE THESIS OF

Kevin R. Caple for the degree of Master of Science in Chemical Engineering
presented on August 30, 2010,

Title: Oxidative Desulphurization of Dibenzothiophene with Tert Butyl Peroxide in a Carbon Nanotube Supported Corona Discharge Microreactor

Abstract approved:

_____

Alexandre F. Yokochi Goran Jovanovic

Sulfur content in fuel is an increasingly important environmental concern. A commonly used method for the removal of sulfur bearing species from fuel is through hydrodesulphurization. However, due to the implementation of Ultra-Low Diesel Sulfur (ULDS), deeper desulphurization techniques must be explored. In this study, a single phase oxidative desulphurization microreactor is crafted for this purpose.

The proposed microreactor is built around the concept of corona discharge. The corona is created through a significant potential difference between a carbon nanotube supported emitter electrode and a stainless steel collector electrode. The current that passes through the two electrodes acts as a catalytic agent for the oxidation of the sulfur bearing species.

Dibenzothiophene and tert-butyl peroxide are mixed with decane into two separate feed streams. The two feed streams are sent through a micromixer and continue into the reactor. The reactor system is activated and current flows within the reaction volume between the two electrodes. The proposed reaction mechanism is similar to that of the photooxidation of dibenzothiophene in which the peroxide is cleaved by the electrical energy and subsequently reacts with the sulfur to form its

oxides, sulfoxides and sulfones, respectively. Due to the high polarity of these products, they are easily extracted from the fuel stream.

Experiments testing the capabilities of the proposed reactor include varying the applied current to the reaction volume, inlet concentrations of both the fuel and oxidant streams, the reactor volume residence time, the post-reactor volume residence time, and the effect of aging upon the oxidant stream.

This proposed microreactor was successfully crafted and the corona successfully discharged between the emitter and collector electrodes. Testing of the reactor's capabilities suggest that the proposed oxidation mechanism is not strictly duplicated within this microreactor system. For this first generation reactor system, a maximum conversion of 68% of dibenzothiophene to its sulfoxide and sulfone has been found. Dissolved oxygen in decane was also found to be a sufficient oxidant source to initiate the oxidative reaction and has been shown to continue to be an oxidant source even in the presence of peroxide.

# Oxidative Desulphurization of Dibenzothiophene with Tert Butyl Peroxide in a Carbon Nanotube Supported Corona Discharge Microreactor

by

Kevin R. Caple

A THESIS

Submitted to

Oregon State University

in partial fulfillment of

the requirements for the

degree of

Master of Science

Presented August 30, 2010

Commencement June 2011

Master of Science thesis of Kevin R. Caple presented on August 30, 2010.

APPROVED:

---

Co-Major Professor, representing Chemical Engineering

---

Co-Major Professor, representing Chemical Engineering

---

Head of the Department of Chemical, Biological, and Environmental Engineering

---

Dean of the Graduate School

I understand that my thesis will become part of the permanent collection of Oregon State University libraries. My signature below authorizes release of my thesis to any reader upon request.

---

Kevin R. Caple, Author

ACKNOWLEDGEMENTS

First and foremost, my thanks go to my parents and brother. They have always been infinitely supportive of the decisions that have led me to this point.

A great thanks to Jake Jones and Eileen Herbert for their help on this project. Eileen was one of the progenitors of this work and, unknowingly, her thesis helped guide and develop my own. Jake was, until his move across the country, a springboard for ideas, compatriot, and coworker as we both worked to finish our eerily similar projects at the same time.

I thank my major professor, Dr. Alexandre Yokochi, for his guidance, professional support, and patience that helped me immensely in the development, implementing and finishing of this degree.

I would like to thank the Advanced Materials and Microtechnology Lab Group under Dr. Yokochi for their support, guidance and help when I needed something that I didn't know how to do. Specifically, Nick AuYueng for helping bounce ideas off of for work on the HPLC, Alex Bistrika for his help garnering SEM images, and Matt Delany for bouncing general ideas off of.

I thank Ratih Lusianti for helping me maintain my sanity throughout the course of this project. Whether trading ideas of both of our theses', forcing me to take a break, keeping me extremely well fed and being an emotional support in times that I needed, I would not have finished this project in either the time or energy had it not been for her.

Thanks go to Tactical Energy systems for funding this project.

TABLE OF CONTENTS

Page

TABLE OF CONTENTS (Continued)

Page

LIST OF FIGURES

LIST OF FIGURES (Continued)

LIST OF TABLES

LIST OF APPENDICES

LIST OF APPENDIX FIGURES

LIST OF APPENDIX TABLES

# Oxidative Desulphurization of Dibenzothiophene with Tert-Butyl Peroxide in a Carbon Nanotube Supported Corona Discharge Microreactor

# CHAPTER 1

# INTRODUCTION

## 1.1 Sulfur Content Regulation

The emission of sulfur bearing compounds from combustion engines leads to the creation of several hazardous chemicals including sulfur dioxide and sulfuric acid. These emissions, due to inefficient combustion and treatment, can be attributed to several environmental risks, including acid rain, deforestation, smog, and global warming, as well as several human health concerns such as cardiovascular disease, cancer, creation of asthmatic symptoms and other respiratory diseases.[1] Several stringent restrictions have been implemented by the Environmental Protection Agency (EPA) in order to remove sulfur bearing compounds from diesel fuels. This Ultra Low Sulfur Diesel (ULDS) program regulates that, as of June 1, 2010, all highway diesel fuel must be ULDS or contain less than 15 parts per million (PPM). Studies performed by the EPA have shown that over 94% of the diesel sold in the United States meets the regulations for ULDS.[2]

## 1.2 Microtechnology

### 1.2.1 Definition of Microtechnology

Microreactors are scaled down reaction systems designed to overcome the obstacles that are presented by large scale applied systems. A microreactor is defined by one of its dimensions (usually labeled as the height or thickness) being within the micrometer length scale. The length and width of the reaction volume can be anywhere from millimeters to tens of centimeters in length. Construction of microreactors is performed through either top-down or bottom-up processes, in which the specific pieces for the microreactor are built or crafted from one side of the system to the other. This crafting process allows for significantly easier and efficient construction and development of several final pieces on a mass scale.

### 1.2.2 Benefits of Microtechnology

<u>Decreasing Dimensions</u>

Scaling down macro sized equipment to the micro scale is performed in order to exploit the physical and chemical differences that are applied between the differences of scale. The first of these is the extremely large surface to volume ratio. Average laboratory and production systems have a ratio between 100 and 1,000 $m^2/m^3$. Microreactors, on the other hand, can have ratios up to and greatly

exceeding 10,000 $m^2/m^3$.[3] These high ratios allow the system to operate with highly efficient heat and mass transfer. This allows for reactions and operations that are enormously exothermic on a macro scale to operate safely and with significantly less heat loss on the micro scale. Diffusion times are dramatically shorter in the smaller volume and the mass transfer limitations can essentially be nullified.[4,5] Indeed, mixing times within smaller micro-mixers can be in the millisecond range.

Increased Efficiency

Due to the size of macro scale units, residence times within a reaction volume can be on the order of hours to days for both photochemical and catalytically driven batch oxidative desulphurization processes. However, on a micro scale, residence times can be reduced to minutes or even seconds. For some chemical reactions on the macro scale, the residence time is much longer than that based upon the kinetics of the reaction. This is due to the poor mixing and minimal contact in batch scale reactions. Microreactors, however, because of their near instantaneous mixing and orders of magnitude smaller reaction volume ensure that the “plugs” sent through the volume are set in highly ideal settings allowing for higher conversion per unit time and increase the selectivity of the reaction as the operational parameters of the microreactors can be controlled much easier than those on the batch scale. This phenomenon also allows for continuous processing in which a constant flow

system is used rather than batch, allowing for simpler operational control over the system.

Numbering Up

A significant issue within the principles of microtechnolgy is that it is unable to match the throughput that more conventional macro scale machinery produces. To match this higher throughput, numbering up is implemented. Rather than have an entire reaction take place in a single piece of equipment, several pieces are joined together. This system sets the unit in both series and parallel allowing for a higher throughput. Numbering up is also used to increase selective conversion and minimize heat lost by softening the reaction conditions, increasing the total efficiency (including energy balancing) of the entire operation.

## 1.3 Goals and Objectives

The primary goal of this work is to develop a microreactor system that has the capability to induce a corona discharge. The reactor's capabilities will be determined by studying the oxidative reaction of dibenzothiophene to both of its subsequent oxides in a mock logistic fuel. The objectives necessary to complete in order to achieve this goal are:

1. Design of microreactor system

2. Development of electrodes necessary for corona discharge
3. Crafting of microreactor system with said electrodes
4. Tests verifying corona discharge in the reaction volume
5. Experiments investigating the capabilities of the proposed microreactor

# CHAPTER 2

# BACKGROUND

## 2.1 Desulphurization

### 2.1.1 Hydrodesulphurization

Hydrodesulphurization (HDS) is catalytic process that uses hydrogen gas to remove impurity compounds containing oxygen, nitrogen, metals, and sulfur from liquid petroleum streams.[6] Sulfur can continue to cause harm when remaining in the finalized product through its combustion to create sulfur dioxide, which causes numerous health and environmental concerns previously discussed. The main reaction for HDS is shown in Figure 2.1. It involves the cleavage of the impurity compound (in this case involving sulfur), resulting in two alkyl groups and hydrogen sulfide gas.

$$R - S - R' + 2H_2 \rightarrow RH + R'H + H_2S$$

Figure 2.1 Hydrogenation of Sulfur Bearing Species

In a typical HDS process, hydrogen rich gas (from pure and recycled sources) is mixed with the liquid petroleum feed and preheated. The feedstock is then sent to a high-pressure, high-temperature fixed bed reactor containing one of several catalysts, often molybdenum based.[7] Within the reactor, sulfur and nitrogen

bearing species (the two that are most likely to be present and poison the noble metal catalysts downstream) are converted into their subsequent alkyl groups and hydrogen sulfide or ammonia respectively. The stream is quenched post reactor and the two streams are separated. Within the gas stream, hydrogen is separated and recycled, while hydrogen sulfide and ammonia are sent to a gas treatment unit. The liquid stream is sent to a stripping column in which hydrogen sulfide and ammonia that have dissolved into the petroleum are removed.[8] Figure 2.2 displays this process.

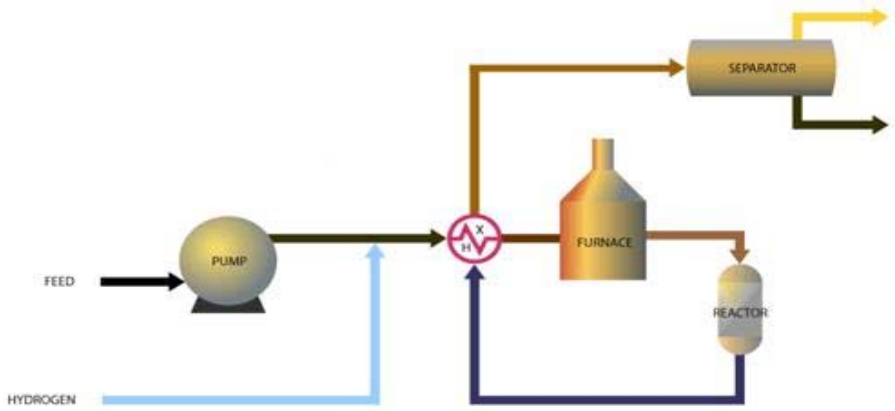


Figure 2.2 HDS Process[8]

There are several inherent disadvantages of the HDS process. The first of these is the cost and danger associated with maintaining the high reactor temperature and pressure. Optimization of catalyst use, regeneration and application, combined

with minimizing the amount of hydrogen needed and used by the reaction is costly and time consuming. Current methods of HDS have difficulty efficiently removing aromatic and other highly steric sulfur and nitrogen bearing compounds because of their relatively low reactivity, even at the high temperatures and pressures commonly used.[7] Research has shown that with each subsequent addition of an aromatic ring, the reactivity of the compound decreases by an order of magnitude.[9] For example, the reactivity of the thiophene family decreases respectively in thiophene (T), benzothiophene (BT), and dibenzothiophene (DBT).[7] It has also been shown that the reactivity is further hindered by the presence of substituents located on the aromatic rings, such as 4,6-dimehtyl dibenzothiophene.[10]

New techniques for hydrodesulphurization include the use of different catalysts in the presence of Grignard reagents. Through the use of palladium nanoparticles and nickel and platinum based compounds, dibenzothiophene has been shown to react to form aromatic compounds with the sulfur removed.[11,12] These include the major product of $\beta$-hydrogens in the 1 and 9 positions as well as the minor product of the R group of the Grignard reagent similarly located on the 1 and 9 positions. This process removes the need for high temperatures and pressure, yet brings up the issue of having several multi-ring aromatic compounds present in the fuel stream.

### 2.1.2 Oxidative Desulfurization

Oxidative desulphurization (ODS) is one of the methods being investigated to replace the hydrodesulphurization process in many industrial plants. The basic principle behind it is to convert the difficult to react thiophenes and other sterically hindered sulfur bearing compound that remain after HDS into their successive oxides.[7] For dibenzothiophene in a photochemical system, light activates an oxidant source (such as a peroxide), which reacts rapidly with the sulfur species to form its subsequent oxides. The benefit of this reaction is to create highly polar oxygenated sulfur compounds which can then be removed in a polar solvent through liquid-liquid extraction leaving a relatively sulfur-free petroleum stream. Oxidative desulfurization has several inherent benefits over its counterpart in HDS. Reaction conditions are much milder, on the order of room temperature and pressure, allowing for easier control over the reaction process and equipment. The processes are generally cheaper than HDS due to the previously mentioned reaction conditions, as well as reduced need for catalysts and other support chemicals such as hydrogen. Also, the production of hydrogen sulfide is severely limited through oxidative methods, meaning that several unit processes built to deal with the dangerous off gas are no longer necessary.

ODS methods can be split into four succinct categories: dual phase liquid, one phase liquid, biological, and other miscellaneous processes. Dual phase liquid ODS describes the processes in which the petroleum stream is mixed with a polar stream containing some sort of oxidant (hydrogen peroxide in water or acetonitrile is commonly used). One phase liquid ODS involves using an organic solvent with an organic peroxide or supported catalysts providing the oxidative power needed. Biological ODS uses specifically chosen bacteria that have an internal mechanism for desulfurization. The final group discusses ODS methods that don't fall under the previously three categories but have been, and continue to be, investigated. Table A.1 in Appendix A shows a summary of the oxidative desulfurization literature reviewed and categorized by the sulfur bearing compounds, the oxidant, catalyst and solvent used, and which of the four previously listed ODS method the literature falls under. These fields of research will be discussed in following four sections.

Dual Phase Liquid ODS Systems

Dual phase liquid ODS consists of applying a non-organic oxidative source to the organic sulfur bearing stream. Commonly this consists of aqueous hydrogen peroxide in the presence of heterogeneous or homogenous catalysts. The literature discusses several heterogeneous catalysts including sodium tungstate, tungsten oxides mounted on zirconium oxides, and palladium, chromium oxide, manganate

oxides, and cobalt/molybdenum alloys mounted on aluminia.[13,14,15] Acetic acid, tungstic acid, sulfuric acid, and formic acid have also been shown to catalyze desulfurization processes.[16-19] Homogenous catalysts used included benzophenone and polyoxometalates.[20-22] All of the previously listed literature sources use hydrogen peroxide as the oxidant source in a polar solvent. These solvents include water, acetonitrile, methanol, dimethyl formadide, and ethanol.[13,14,16,23] The use of activated carbon is suggested to yield oxidation of sulfur bearing materials in combination with a hydrogen peroxide-formic acid system.[19]

Single Phase Liquid ODS Systems

Single phase liquid ODS systems consist of applying an organic oxidant supply to the petroleum stream. This is often accomplished by using organic peroxides such as tert-butyl hydroperoxide (TBHP). TBHP has been found to be an effective single phase oxidant in combination with titanium based, and molybdenum, chromium, tungsten, vanadium, niobium, and zirconium based catalysts.[24,25] One group has used TBHP and cumene hydroperoxide in various water immiscible organic solvents catalyzed by Celite deposited hemoglobin, myoglobin, and cytochrome c, to show that the cumeme hydroperoxide was able to oxidize dibenzothiophene using all three hemoproteins, reaching 91% oxidation with cytochrome C.[26]

Biological ODS Systems

There has been a great deal of research being focused on replacing chemical processes with biological ones. The idea behind it is that, by using bacteria, small plants, and other easily maintained and grown organisms, the processes will become significantly cheaper, more eco-friendly and reusable. Research has been undertaken to apply biological systems into oxidative desulfurization. This researched is backboned by the internal processes of bacteria. Dibenzothiophene is most often used in these studies as it is highly resilient against HDS. The *rhodococcus* sp. Strain ECRD-1 has shown 38% desulfurization of middle distillate oil.[27] The *gordona* strain CYKS1 has shown up to 50% removal of sulfur bearing compounds.[28] Despite these studies, biological ODS is viewed as a relatively ineffective method for removing sulfur from fuel streams. In order for these systems to garner support and funding, they must be combined with some other process such as HDS and further research into increasing conversion rate, stability and cost effectiveness must be explored.[27]

Miscellaneous Systems

Several unique approaches towards ODS involve techniques that do not fall under the previously listed methods. Of the miscellaneous methods, one of the more common desulfurization techniques involves photo-oxidation. Photo-oxidation involves the creation of free radicals of one of the major reactive species via

irradiation by some kind of energy source (UV light being the most common) in the presence of a photocatalyst.[29] The hydroxyl radical is commonly used, formed through the cleavage of hydrogen and other peroxides. Within these photooxidative processes, the major differences within the literature prove to be the catalyst used. However, whether using titanium dioxide, TS-1, or MOPDPP$^{+}BF_4^{-}$ moderate conversion of sulfur bearing species have been found.[30-32] However, these processes are limited because of the irradiation times necessary in order to achieve high conversions and the destructive nature of the reaction.

A novel approach to the subject of ODS involves the use of ozone, hydrogen peroxide, and ionic liquids.[33] An ionic liquid is essentially a salt in the liquid state and are generally applied as very powerful solvents and electrolytes. In this study, ozone and hydrogen peroxide were reacted within an ionic liquid and fuel mixture to form hydroxyl radicals. These hydroxyl radicals attack the sulfur of the thiophene and after a subsequent removal of the hydrogen, bond to the sulfur. This first oxide is usually called “sulfoxide” while further oxidation produces a dioxide called a “sulfone.” The oxidized species can then be extracted into the ionic liquid phase. With the combination of the ionic liquid, ozone, and hydrogen peroxide, the sulfur removal was found to be 98.6%. Another novel approach involves the catalysis of dibenzothiophene through contact with a silica gel matrix.[34] Through varying pH and organic solvent at moderate temperatures, the authors were able to show that, in

acidic conditions, dibenzothiophene was oxidized at a high conversion when decalin and tetralin were used as a solvent.

All of the previously discussed methods, in all four categories, require two things: an oxidative source and some sort of catalytic process to initiate the reaction. While some of these may prove to be cheaper, more efficient methods for deep desulfurization, they would still require several unit processes in order to produce the pure fuel. Also, the need for catalyst replacement, recharging, and optimization on a case by case basis drive the costs for several of these systems up.

## 2.2 Corona Discharge

### 2.2.1 Physics of Coronas

A corona is an electrical discharge created due to a high potential difference between two conductive electrodes. This high potential creates a gradient across a neutral fluid (as a gas, air; as a liquid, any organic alkane suffices) by ionizing the fluid and creating plasma around the electrode.[35] After a certain amount of time, the plasma passes electrons into areas of weaker potential allowing, if desired, current to flow between the discharge electrode and ground electrode. Applying a positive corona discharge to a system entails having a discharge electrode with a very sharp point. The purpose of this is to maximize the potential gradient in one localized area, as to initiate the ionization of the neutral fluid. As the size of the

point gets smaller, the gradient and ionization rate increases. A positive corona can be defined as when the curved electrode with the small point is positive with respect to the flat electrode while a negative is the reverse of this. Positive and negative coronas have distinctly different physical properties which are a reflection of the difference in mass between the positively charged ion flow created by the positive corona and the electron flow created by the negative corona. These physical differences result in widely different results when applied to a physical system.[36]

Several compounds can be used to create the positive corona. Platinum/rhodium, stainless steel needles, stainless steel rings, platinum and nickel chromium have all been studied in impurity or pollutant removal.[37-41] Carbon nanotubes have demonstrated efficient electrical emission from nanotube based gas phase systems.[42,43] The use of carbon nanotubes for the application of corona discharge is one of the primary focuses of this study.

### 2.2.2 Application of Coronas

Corona discharge, either positive or negative, can be applied in any gas or liquid setting. Currently, a majority of the research has been performed on applying the corona within the gas phase and usually with air as the medium. Air is an excellent medium as it has an oxidant source (oxygen), a carrier gas (nitrogen), and is readily

available. In some situations, however, the radicalization of oxygen instigates the creation of ozone which possesses highly destructive properties. Often, water is used in lieu or in combination with air to serve as a hydrogen source and a radical source for creation of hydroxyl radicals. Unfortunately, as with any radical reaction, the products are difficult to predict and select. The reaction between the hydroxyl radical and toluene has shown to produce benzoic acid, benzaldehyde, benzyl alcohol, 4-methyl phenol, and 4-methyl benzoic acid.[44] Methanol and dimethyl sulfide react with radicalized water to form methanol, carbon monoxide, nitrous oxide, nitric oxide, formaldehyde, ethane, and sulfur dioxide.[45] Other compounds that corona discharge is applied in the gas phase to remove include acetone and iso-propyl alcohol, n-hexane, i-octane and trichloroethane, vinyl chloride.[46-48]

Despite the heavy level of attention paid to the application of corona discharge in the gas phase, several practical uses for it have been explored in the liquid phase. In application in liquid phase, the carrier fluid can also be used as the radical source, such as water. Indeed, the use of non-thermal plasma for water treatment as a unit process within a water or waste water treatment plant is one application that is being thoroughly explored due to the amount of pollutants in the water that are not removed by other processes.[48] A combination of gas and liquid coronas can be used for the reaction of chemicals such as phenol that have a moderate vapor pressure.[35] In a case such as this, the streaming corona passes through the liquid, a liquid/gas

interface, and into the gas to the receiving electrode.[49] Bubbling gas into a liquid is a novel approach in which the gas reactant is introduced to the reactor directly beneath the discharge site.[50] The potential gradient will ionize the gas and allow liquid-gas interactions to help progress certain reactions.

# CHAPTER 3

# MATERIALS AND METHODS

## 3.1 Chemicals

Dibenzothiophene (>98% Fluka Chemical Company), decane (>99.9%, TCI), tert-butyl peroxide (98%, Sigma Alrich), dibenzothiophene sulfoxide (MP Biomedicals), dibenzothiophene sulfone (97%, Sigma Aldrich), acetonitrile (GC grade, Fisher Scientific) and water (HPLC grade, Mallinckrodt Chemicals) were purchased from chemical suppliers and used as received without any further alteration.

Materials for the development of the micro-reactor system, including Dow Corning Solvent Resistant Sealant 730 and silver epoxy (MG Chemicals), were obtained and used as received. Carbon nanotubes were produced using a vertical thermal reactor employing an alumina supported iron oxide catalyst with ethylene gas as a carbon source. Prior to use, the nanotubes were cleaned via digestion with concentrated sodium hydroxide followed by pH neutralization with 1M hydrochloric acid. The nanotubes were filtered and dried in a convection oven at ~100°C overnight.

The synthetic fuel streams consisted of a stock solution of dibenzothiophene with a concentration of approximately 4226 PPM in decane. The oxidant stream consisted of 5515 PPM tert-butyl peroxide in decane.

## 3.2 Chemistry

The oxidative reaction observed in this study uses tert-butyl peroxide and dibenzothiophene as base reactants to form dibenzothiophene sulfoxide and dibenzothiophene sulfone.

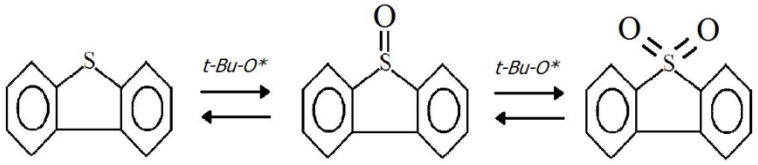


Figure 3.1 Oxidation of Dibenzothiophene (DBT) to DBT Sulfoxide and DBT Sulfone

The proposed oxidation mechanism occurs via tert-butoxyl radicals, which are formed when tert-butyl peroxide is exposed to enough energy (in this study, electrical).

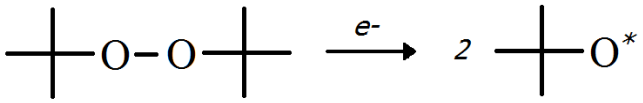


Figure 3.2 Proposed Radicalization of *tert*-butyl peroxide to *tert*-butoxyl radicals

This is the proposed mechanism based off of previous studies of dibenzothiophene oxidation using peroxides.

## 3.3 Reactor Development

A 76.2 x 24.4 x 2 millimeter stainless steel piece is used as one side of the proposed electrical circuit and reactor. This piece has six one sixteenth inch diameter holes drilled in it for inlet and outlet tubing placement. Dow Corning Solvent Resistant Sealant 730 is used to completely cover the stainless side of the metal piece. Previous materials including PDMS and Dow Corning Heat Resistant Sealant were attempted to create the reaction volume, but were disregarded because of their solubility and weakness against organic solutions. Immediately after covering, a knife razor was used to even the sealant, shown in Figure 3.3

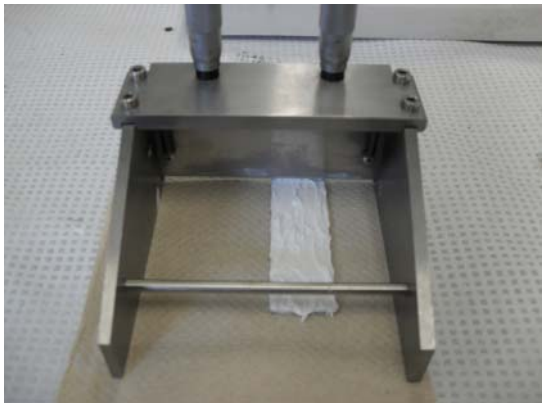

Figure 3.3 Image of Knife Razor used to level Sealant on Steel Surface

The sealant is allowed to cure overnight in order to carve out the reaction volume. The reaction volume is of parallelogram form with a base length of 50 millimeters and a width of twenty millimeters. To fully clean the reaction volume, the metal was scrubbed with steel wool and washed with toluene. The final product is illustrated in Figure 3.4.

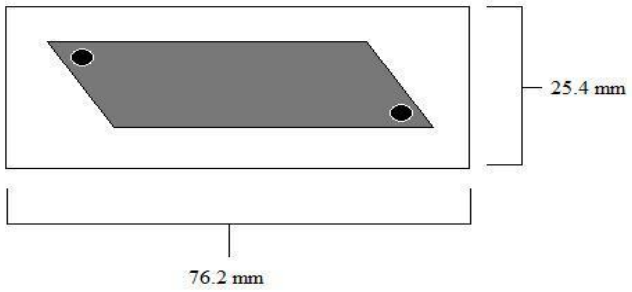


Figure 3.4. Illustration of bottom electrode with dried sealant and reaction volume removed

The other electrode comprising the circuit is to be composed of a mixture of conductive silver epoxy and carbon nanotubes. Other methods attempted to create the conductive glass electrode comprised of electroless nickel plating upon the raw glass and the use of silver pens, often used in circuitry, as a way to create a link between a power supply and the carbon nanotubes. Both methods were discarded because they did not allow simple application of carbon nanotubes to the electrode. Approximately one hundred milligrams of the nanotubes are mixed with two milliliters of silver epoxy thoroughly before being spread onto a 3”x1½” glass microscope slide. The mixture is spread as evenly as possible and allowed to dry overnight. Sandpaper was used to roughen and even the surface of the electrode and allow for a flat surface with more nanotubes exposed. Figure 3.5 A/B/C show SEM images displaying the carbon nanotubes as they appear on the surface of the electrode. The images show that the nanotubes have diameters on the order of 25 to 40 nanometers and lengths in the hundreds of nanometers. The reasonably

evenly spaced nanotubes is desirable as it allows for more opportunity of corona discharge and activation of the oxidation reaction.

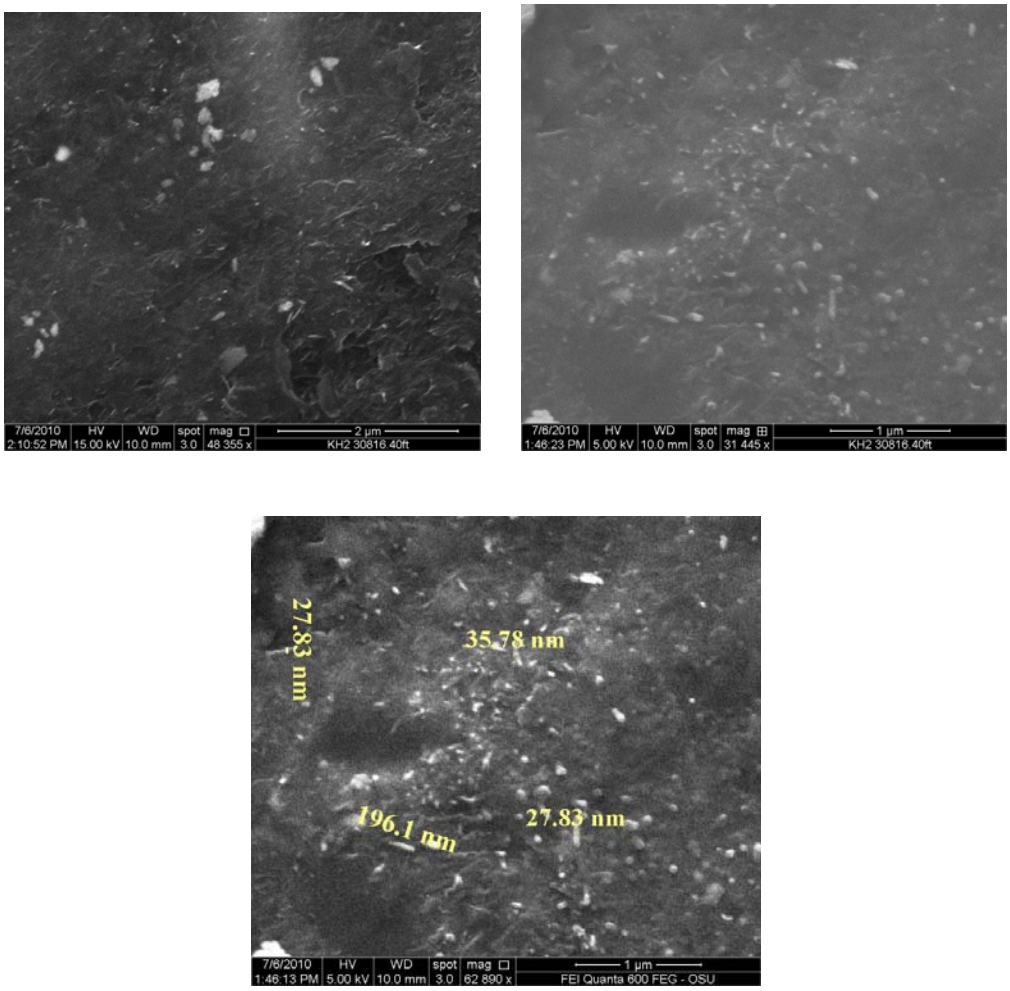


Figure 3.5 A (top left), B (top right), and C (bottom): SEM images of carbon nanotubes mixed with silver epoxy

Once both pieces of the electrode are dry, they are both placed into a Technics PlanarEtch II Oxygen Plasma Etcher for 35 seconds at 24 W for activation. The etch

removes the top “inactive” layer of both the dried sealant and epoxy mix. Immediately following the etch, the pieces are stuck together and placed under weight overnight to ensure contact. Any leaks that were found are plugged with solvent resistant sealant. Figure 3.6 shows the finalized microreactor (A), as well as the side dimensions (B).

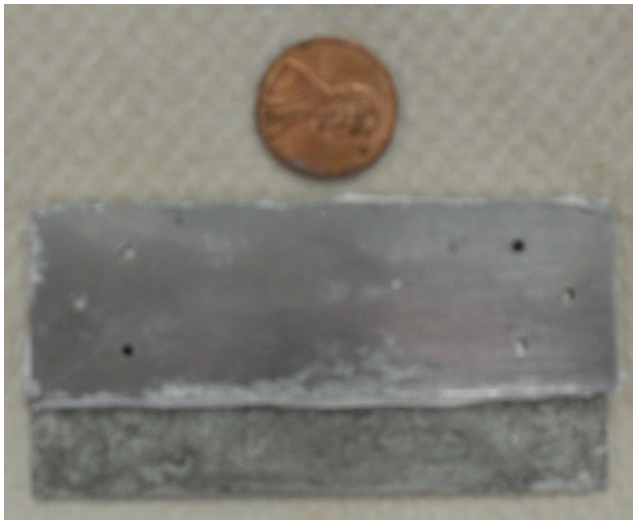


Figure 3.6 A/B. Finalized reactor (above) and illustrated side dimensions drawn to scale (Below)

PEEK tubing (.02” ID) is used to transport the reactants to the microreactor. Inlet and outlet tubes are placed in the drilled 1/16$^{th}$ inch diameter holes on the metal

slide with O-rings to ensure no leaking occurs. As a further precaution against leaking and back pressure, the tubes are sealed into the reactor with more solvent resistant sealant and allowed to dry. Two New Era Pump Systems syringe pumps were used to deliver the two streams (dibenzothiophene in decane and tert-butyl peroxide in decane) to the micro-reactor system. Orange PEEK tubing was used to connect the two syringes to a micromixer, ensuring that the two streams were fully mixed before reaching the reactor.

The reactor is mounted onto a plastic polymer mount with influent and effluent holes previously drilled, in order to prevent unintentional shorting of the circuit. A Life Tech Model 4001P power supply is used to apply current and voltage to the microreactor system. In order to manage the large amounts of voltage applied to the system, a resistor bank composed of “ballast” resistance is created. Figure 3.7 shows the P&ID for the experimental system for a positive corona discharge electrochemical system.

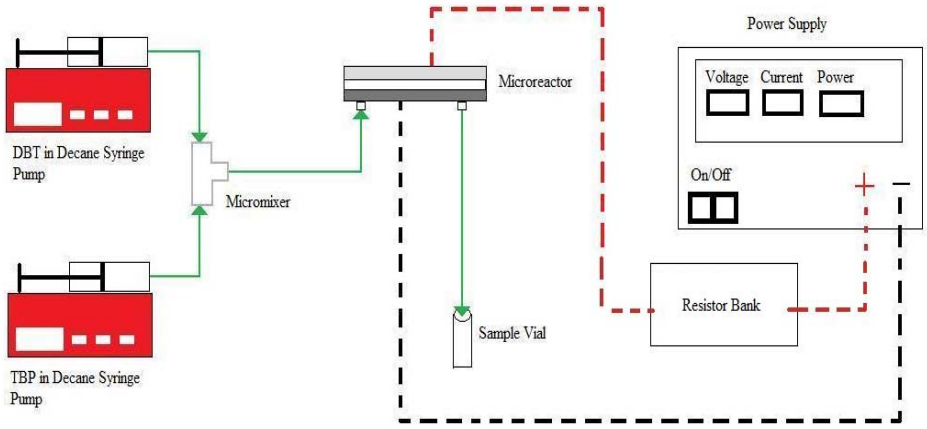


Figure 3.7 Experimental P&ID

The ballast resistance is of the form of two sets of five 470 kΩ resistors in parallel. This yields a ballast of 94 kΩ per set and 188 kΩ for the entire ballast bank. This allows higher currents to reach the microreactor system without overloading it with high voltages.

## 3.4 Experimental Variables

In the course of this study, five experimental variables were examined: influent dibenzothiophene concentration, influent peroxide concentration, total reactor volume residence time with varying flow rate ratios of peroxide to dibenzothiophene, post-reactor residence time, and applied current to the reactor. Table 3.1 lists the different experiments performed, showing the variable change (listed in bold) as well as the values of the standards.

Table 3.1 Experimental Variables

| Experiment | DBT Concentration (Stock – 4226 PPM) | Peroxide Concentration (Stock – 5515 PPM) | Peroxide:DBT Flow Rate Ratio | Effluent Residence Time | Current |
|---|---|---|---|---|---|
| 1 | 4226 PPM | 5515 PPM | 1:1 | 1.015 minutes | **.16-8.66 mA** |
| 2 | **5-90% Standard** | 5515 PPM | 1:1 | 1.015 minutes | 2.56 mA |
| 3 | **1-5% Standard** | 5515 PPM | 1:1 | 1.015 minutes | 2.56 mA |
| 4 | 105.65 PPM | **200-2000% Standard** | 1:1 | 1.015 minutes | 2.56 mA |
| 5 | 105.65 PPM | **0-70% Standard** | 1:1 | 1.015 minutes | 2.56 mA |
| 6 | 4226 PPM | 5515 PPM | **2:1** | 1.015 minutes | 2.56 mA |
| 7 | 4226 PPM | 5515 PPM | **4:1** | 1.015 minutes | 2.56 mA |
| 8 | 4226 PPM | 5515 PPM | **8:1** | 1.015 minutes | 2.56 mA |
| 9 | 4226 PPM | 5515 PPM | 1:1 | **.20-4.05 minutes** | 2.56 mA |
| 10 | 4226 PPM | **5515 PPM** | **2:1** | 1.015 minutes | 2.56 mA |

## 3.5 Analytical Method

An HP 1090 high pressure liquid chromatograph (HPLC) was used to determine effluent concentrations of all three major species (dibenzothiophene, dibenzothiophene sulfoxide, and dibenzothiophene sulfone). Calibration curves of all three major species were created via use of the auto-sampler that is built into the

HPLC used. Three samples of stock solutions with a known concentration of the three major species were placed into the auto-sampler. The HPLC was programmed to remove 1, 2, 3, 4, 5, 10, 15, 20 and 25 µL of each sample and inject it into the column. Each species, based on its unique molecular structure, has a specific retention time in the C18 column used. This will allow for differentiation between the three when the experimental samples are run. The results from the different volume injections, along with a known concentration, can directly relate the number of moles in a system to the peak area it produces. Figures 3.8, 3.9, and 3.10 show the calibration curves relating the moles of dibenzothiophene, dibenzothiophene sulfoxide, and dibenzothiophene sulfone to peak area, respectively.

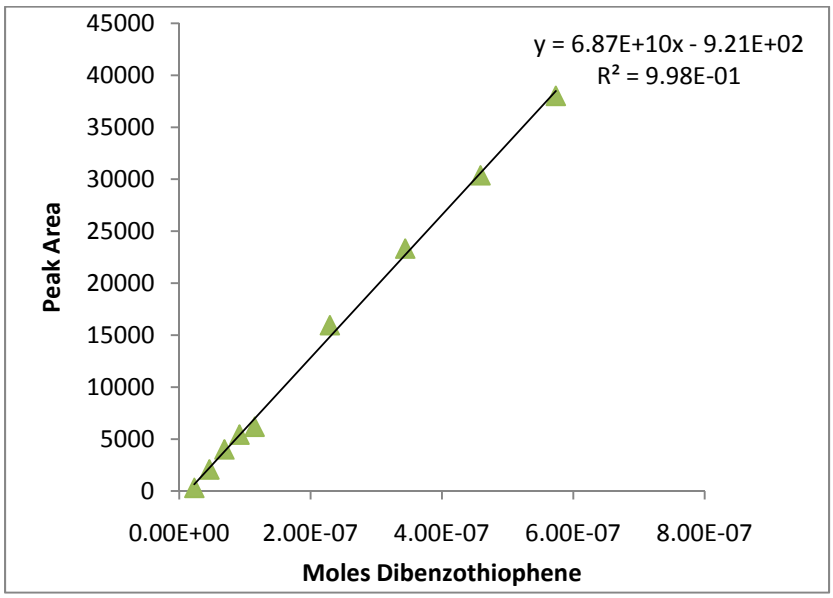


Figure 3.8: Calibration Curve of Dibenzothiophene

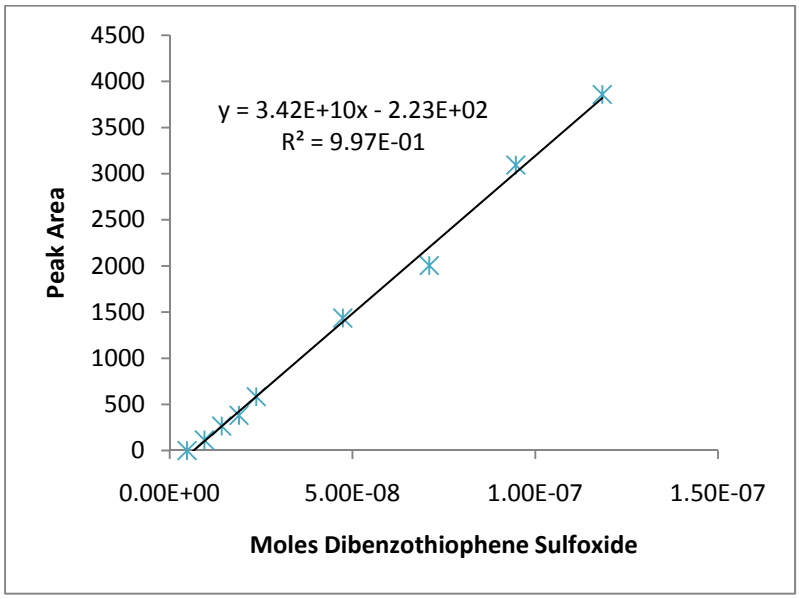


3.9: Calibration Curve for Dibenzothiophene Sulfoxide

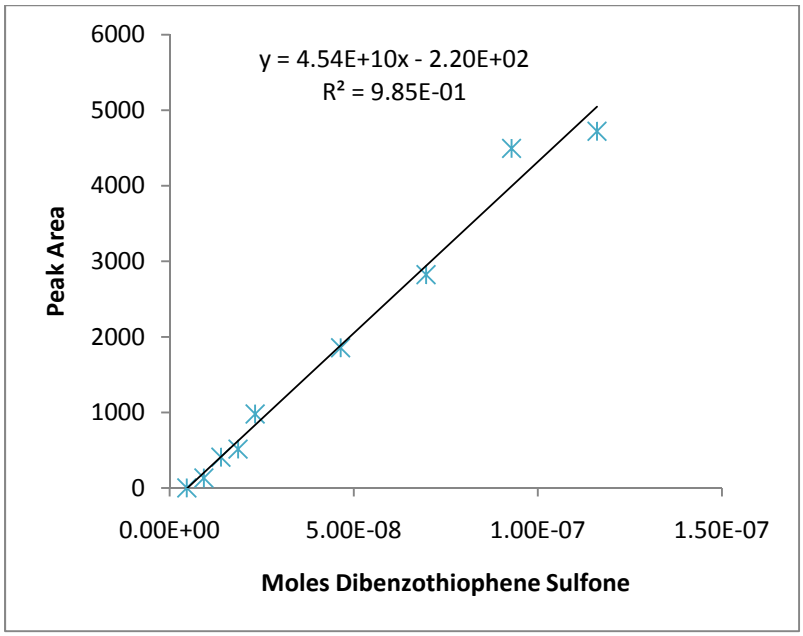


3.10: Calibration Curve for Dibenzothiophene Sulfone

Using the conditions described previously, the peaks for dibenzothiophene, dibenzothiophene sulfoxide, and dibenzothiophene sulfone have retention times of approximately 5 minutes, 4½ minutes, and 3½ minutes, respectively.

# CHAPTER 4

# RESULTS AND DISCUSSION

Experiments were conducted using the methods previously described in Chapter 3 and following the individual protocols listed in Appendix C. The content of the effluent stream, moles and mole percent of dibenzothiophene (DBT), dibenzothiophene sulfoxide (DBTO), and dibenzothiophene sulfone ($DBTO_2$), are listed in Appendix D. Table 3.1 shows the experimental variables. Plots are fitted using natural log in order to display their trends with greater magnitude.

## 4.1 Reactor Testing

Several characteristic tests were performed on completed version of the designed microreactor. These include determining the impedance between the two electrodes with air and decane in the reaction volume, the turn on voltage or the voltage necessary to discharge the corona, and the voltage drop across the ballast resistance. The impedance between the two electrodes was tested using a standard multimeter with its electrodes placed on opposite sides of the reactor. In the successfully crafted reactor, the impedance was found to be greater than the multimeter was capable of reading with both air and decane in the reaction volume.

The final two experiments in testing the reactors involved the necessary voltage required to initiate the corona discharge across the reaction volume and the voltage drop that occurs across the ballast resistance. Figure 4.1A shows the voltage/current plot and Figure 4.1B shows a blown up portion of that plot around the turn on voltage.

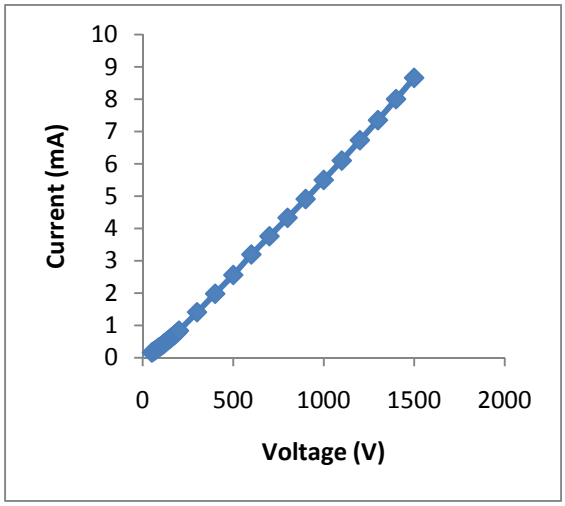


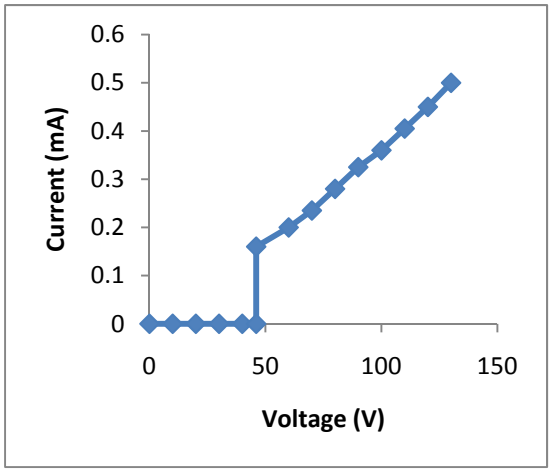


Figures 4.1A/B: V/I plots displaying turn on voltage of proposed microreactor

This experiment displayed that a positive corona microreactor system was successfully crafted and the designed circuit was closed between the two electrodes encasing the reaction volume. A turn on voltage of approximately 46 V was found to activate the corona system, with a maximum voltage of 1500 V before the ballast resistance used to maintain the current levels began to fail. As compared to other, more conventional system that require upwards of 15 kV to activate, this reactor system competes extremely well.

Due to the amount of power being supplied to the reactor system, ballast resistance was necessary in order to keep the circuit from shorting. However, the ballast resistance created a vast difference in the voltage generated by the power supply and that applied to the reactor. Figure 4.2 shows this relationship.

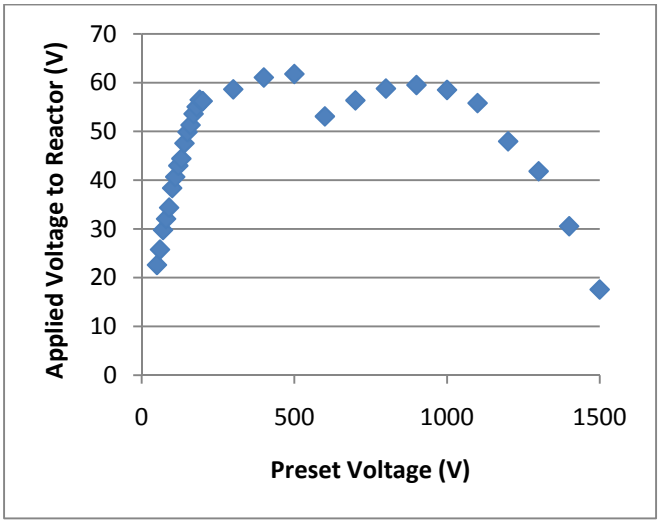


Figure 4.2:. Voltage Drop across Ballast Resistance

The maximum applied voltage to the reactor was approximately 63 V, produced by a preset voltage of 500 V. The substantial drop in applied voltage after 1000 V of preset voltage increases can be attributed to the ballast resistor bank beginning to fail, causing the electrical energy to be released as heat within the ballast resistance.

Despite the performance of the proposed reactor, several issues still remain. This first generation reactor lacks a degree of reproducibility, as the technique to create it does not allow for disassembly without destroying the reactor system. This proves difficult should the reactor develop internal problems. The initial reactor use for the ten experiments previously described eventually developed issues in which the system no longer produced a corona discharge current across the reaction volume. In order to understand what had happened, this reactor was taken apart and subsequently destroyed in order to discover that the two electrodes had shorted due to excess current being applied to the reaction volume. Upon inspection, dark discoloration similar to burning was discovered on both electrodes. This suggests that too much power had been supplied to the reactor and caused a short, crippling or destroying the reactors capabilities.

## 4.2 Estimates and Current

Based off of previous work done using a similar experimental set up, several initial assumptions were made. The mole ratio between peroxide and DBT was 4:1,

assuming two molecules of peroxide were responsible for oxidizing the DBT to its sulfoxide and sulfone, respectively. This follows the line of thinking that an increase in the amount of the peroxide within the system ultimately leads to a higher effluent presence of both oxidized species. An increased residence time within the reactor volume and higher currents were assumed to increase effluent concentrations of both oxidized species.

The novel approach that this work studies involves the applying current to a microreactor in order to initialize an oxidative reaction. Of the performance parameters studied, current and the methods crafted to apply it to the system are the most significant. Several different voltages were applied across the previously described “ballast resistance” to garner currents ranging from 0.16 to 8.66 mA across the reaction volume. Figure 4.3 shows the effluent conversion of DBTO and $DBTO_2$ across the current range.

This data shows an initial turn on conversion (with respect to the turn on voltage of ~50 V) of 28.71% and a maximum conversion located at the maximum applied current of 35.10%. Both the DBTO and $DBTO_2$ show highly positive trends with respect to increasing current, though the $DBTO_2$ especially so, with a slope nearly an order of magnitude larger than that of DBTO.

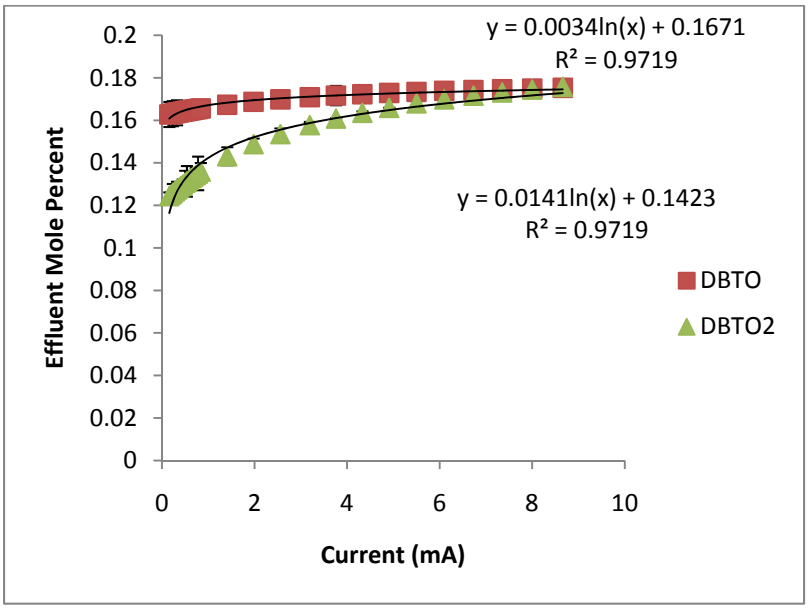


Figure 4.3 Effluent Mole Percentage of DBTO and $DBTO_2$ for Varying Applied Current

Intuition states that the more electrical energy introduced into the system, the more radicals are produced to create more oxidized species. The results of this experiment coincide very well with the initial thoughts on how this experiment would behave. The current supplied to the reaction volume was limited by the ballast resistance and the thickness of the reaction volume. As previously stated, if current is supplied in excess, the circuit becomes shorted and the corona is no longer able to discharge between the electrodes. If reactor thickness is held constant, the only way to increase the amount of current supplied to the reactor is to create a stronger ballast resistance. This is accomplished by setting several high kilo-ohm resistors in parallel with each other allowing the high amounts of power

being supplied by the reactor to dissipate across the resistor bank and not short the reactor. If the ballast is to be held constant, shortening the distance between the electrodes will increase the current density (mA/m), effectively putting the same amount of power into a smaller volume.

## 4.3 Reaction Volume

To ensure that the bulk of reaction occurred within the reactor volume, an experiment was performed in which the effluent channel tube length was varied from .05 m to 1 m. This varied the effluent tube residence time from 12 seconds (.20 minutes) to 243 seconds (4.05 minutes). The remaining variables (concentration, flow rate, applied current) were held constant as to determine if the effluent tube length contributed to the reaction in any way. Figure 4.4 indicates the effect of effluent channel tube length on the effluent conversion of the sulfoxide and sulfone.

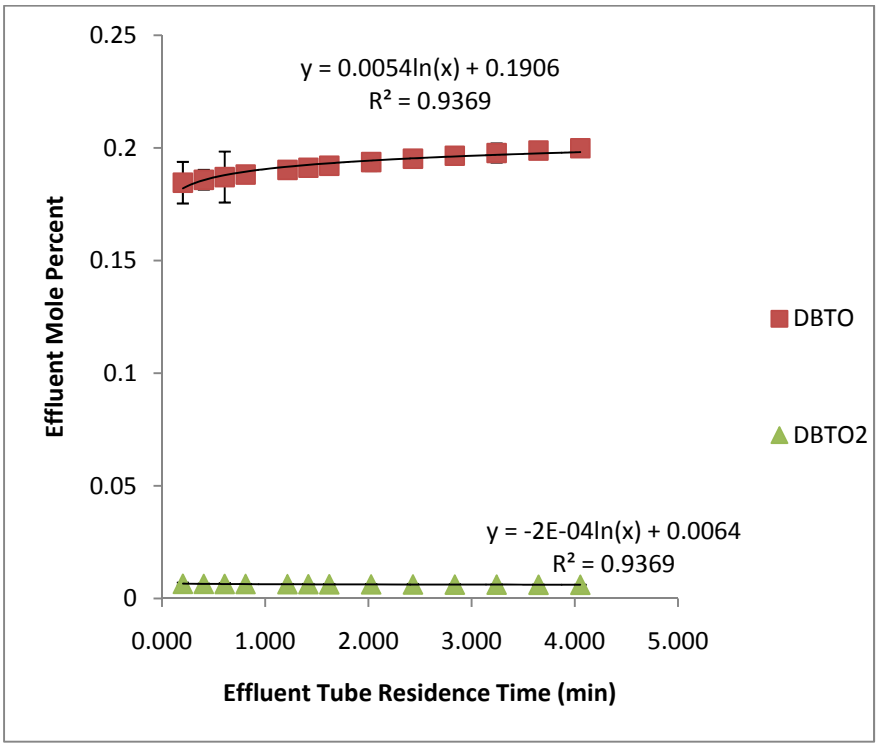


Figure 4.4 Effluent Mole Percentage of DBTO and $DBTO_2$ based on Effluen Tube Residence Time

Figure 4.4 displays the small effect that the effluent tube residence time has on total conversion. The larger increase in DBTO can be attributed to the quenching of the radical reaction. This experiment shows that very little oxidation occurred once the mixed sulfur and oxidant streams left the reactor volume. The oxidation that did occur was such a scale that it appears to be the quenching of any remaining radicals within the system.

## 4.4 Influent DBT Concentration

Two experiments were peformed, evaluating the effects of influent dibenzothiophene concentration on the conversion of DBTO and $DBTO_2$. The first experiment involved dilutions of the stock 4226 PPM dibenzothiophene from 5% to 90%. Figure 4.5 shows the effluent mole percent plot of this experiment.

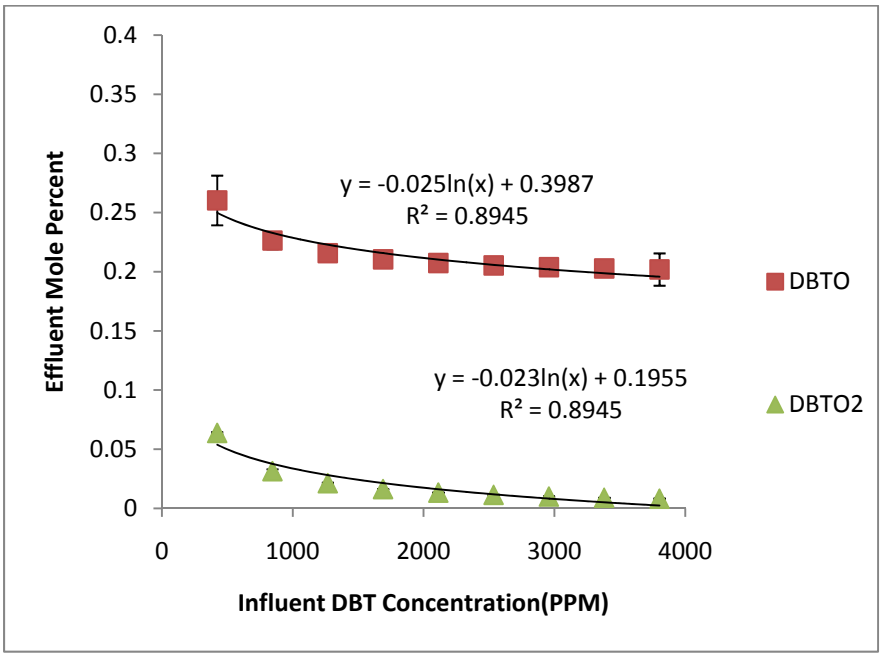


Figure 4.5 Effluent Mole Percentage of DBTO and $DBTO_2$ for Varying Influent DBT Concentrations

This plot shows a clear decrease of conversion of both DBTO and $DBTO_2$ as the influent concentration of DBT strengthens. This would give rise to the reaction being best suited to run at highly dilute solutions of sulfur bearing compounds, as total conversion is higher at more dilute influent concentrations. The relatively high

conversion of DBT to its oxides at lower influent concentrations led to the next experiment in which further dilutions (1%-5%) of the standard were employed. Figure 4.6 displays the effluent mole percent and moles, respectively, of this experiment.

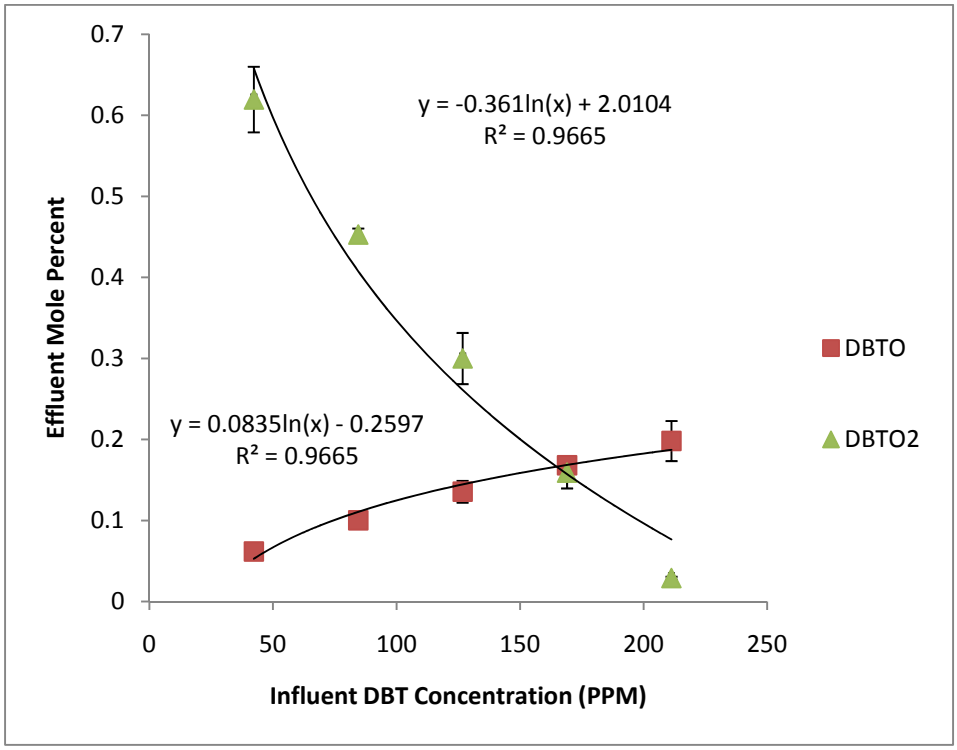


Figure 4.6 Effluent Mole Percentage of DBTO and $DBTO_2$ for Highly Dilute Influent DBT Concentrations

The first point, at 42 PPM, is the highest total conversion found in this work at 68% (62% $DBTO_2$/6% DBTO). This high conversion is attributed to the small amount of

DBT present in the influent stream. Because of this, the formation of one molecule of DBTO or $DBTO_2$ is more significant than in other experiments.

The experiment testing the effects of influent DBT concentration is done because, in an applied refinery setting, the influent streams would have varying concentrations of sulfur. Both experiments showed increasing conversion to DBTO and $DBTO_2$ as the influent concentration decreased. The highest amount of $DBTO_2$ produced was found in the most dilute experimental run with an influent concentration of approximately 50 PPM DBT. This point also corresponded to the highest conversion of $DBTO_2$ of ~60%. However, the converse is true for DBTO, where the highest amount of DBTO produced occurred at the highest influent concentration of DBT, around 4000 PPM. Yet, this point only corresponded to a production of around 20%. The difference in the productions of DBTO and $DBTO_2$ suggest that more of the first oxide will be produced at high influent DBT concentrations while more of the second oxide will be produce at low influent DBT concentrations. As sulfur removal in logistic fuels often consists of liquid-liquid extraction, the production of the second oxide is more favorable, as it produces a more polarized molecule to be extracted into a polar solvent.

## 4.5 Influent Peroxide Concentrations

Two experiments were performed measuring the change in effluent conversion of DBTO and $DBTO_2$ based upon a change in the influent concentrations of *tert*-butyl peroxide. The first experiment uses peroxide concentrations ranging from 11,000 to 110,000 PPM or 2 to 20 times the standard 5515 PPM peroxide. The following figure displays the effluent conversion determined from this experiment.

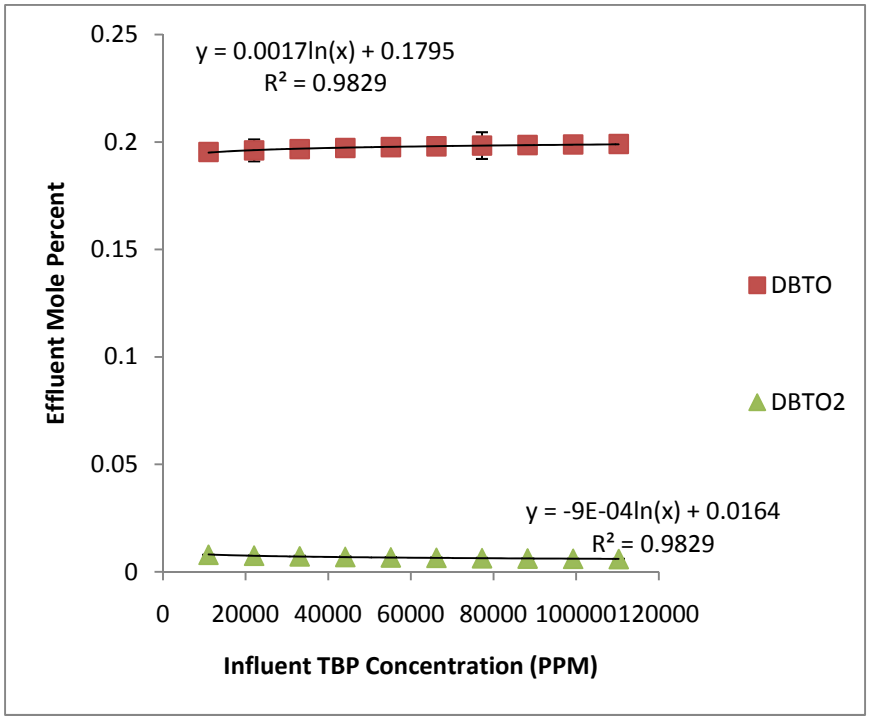


Figure 4.7 Effluent Mole Percentage of DBTO and $DBTO_2$ with Highly Concentrated Peroxide

This previous experiment shows very little change in conversion over the high concentration range. This is counter-intuative to the initial estimates as to the progression of the reaction in which the presence of more peroxide in the system would directly correspnd to a higher conversion. In order to help discern the general

workings of this reaction and garner the full breadth of capabilities of the reactor system, dilutions of the standard peroxide solution were made, ranging from 0 to 70% of the stock peroxide solution. Figure 4.8 shows the respective effluent conversion and number of moles of DBTO and $DBTO_2$

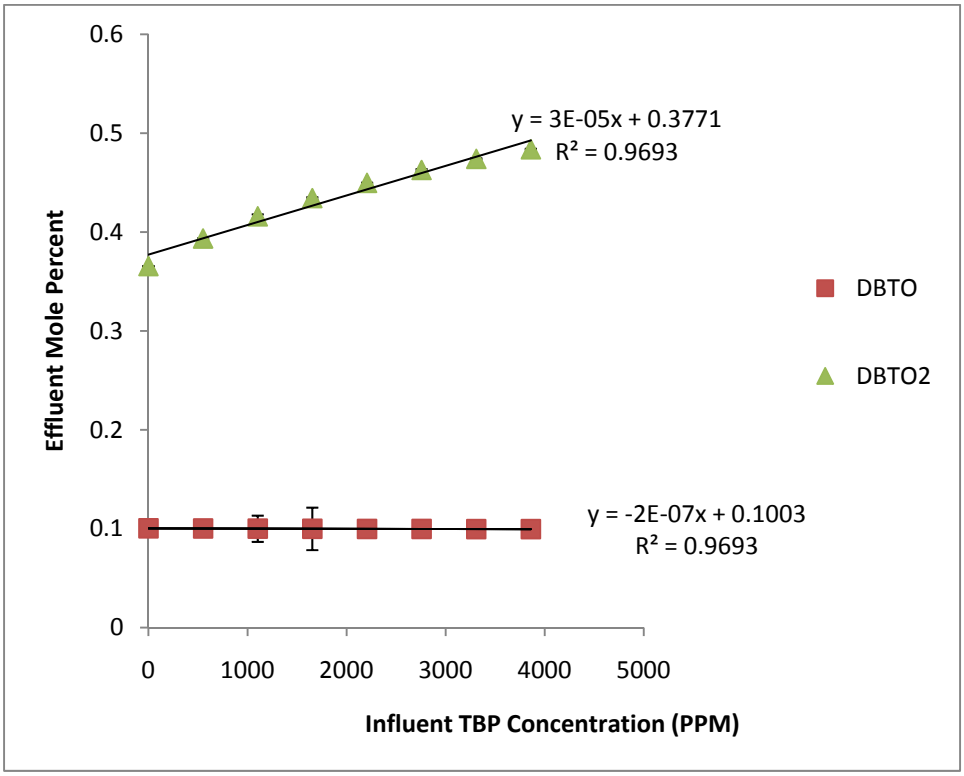


Figure 4.8 Effluent Mole Percentage of DBTO and $DBTO_2$ with Dilute Peroxide

The previous plot show a very high conversion to $DBTO_2$ and a relatively constant, but still noteworthy, conversion of DBTO across the peroxide concentration range. The inlet concentration of DBT was substantially less than that of the previous peroxide concentration experiment. This dilute feed stream, as shown by previous

experiments, suggests that dilute DBT produces a higher oxidation. The significance of this plot, however, lies in the first point, in which no peroxide is introduced and the total conversion amounts to 47%. Mass balances within this experiment show that 87% of the available oxygen dissolved in the feed stream was used to make the final products. It has also been found that, while peroxide appears to be a more favorable oxidant source, the dissolved oxygen continues to serve as an oxygen source.

Intuition and previous work[31] suggested that the addition of more peroxide into the reaction volume would ultimately lead to a higher conversion as there was more of an oxidant source for the same amount of sulfur. Based on the previous experiment varying the influent DBT concentration, dilute (~200 PPM) DBT was used within this set of experiments. The application of extremely high concentrations of peroxide yielded relatively similar results, though the molar ratios varied from 160:1 to 3200:1, peroxide to DBT. This high of a molar ratio proved to show very little change over the concentration range so the converse was tried. Dilutions, ranging from 0 to 70% of the standard (yielding molar ratios of 0:1, then 16:1 to 112:1), were used to study substantially smaller molar ratios. The results of the dilute peroxide experiment proved promising producing high conversion and amounts of $DBTO_2$ and moderate conversion and amounts of DBTO. This experiment also displayed a promising point for future work in which a relatively high conversion was found for

the reaction which carried no peroxide into the reaction volume. Speculation for this point leads to the idea of using dissolved oxygen in the logistic fuel as an oxidative source rather than introducing peroxide.

## 4.6 Residence Times

To further test the capabilites of the designed reactor, three experiments were performed varying the resdience time within the reaction volume at three different flow rate ratios. Experiments were performed with flow rate ratios of 8:1, 4:1, and 2:1, peroxide:dibenzothiophene. Initial flow rates were used (80 microliters per minute peroxide and 10 microliters per minute dibenzothiphene, for example) and then changed at their respective ratios across the residence time spread. These experiments will help continue to help determine the effects of varying peroxide and dibenzothiophene concentrations while simultaneously displaying the effect of increased exposure to the corona dischage. Figures 4.9, 4.10, and 4.11 show the results of the 8:1, 4:1, and 2:1 peroxide to dibenzothiophene flow rate ratio experiments.

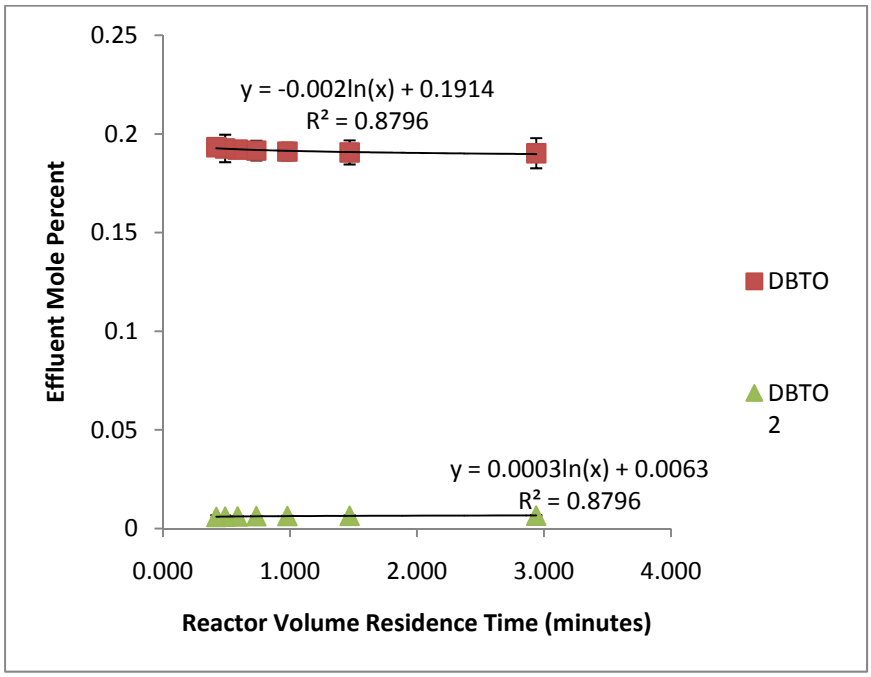


Figure 4.9 Effluent Mole Percentage of DBTO and $DBTO_2$ with 8:1 Flow Rate Ratio

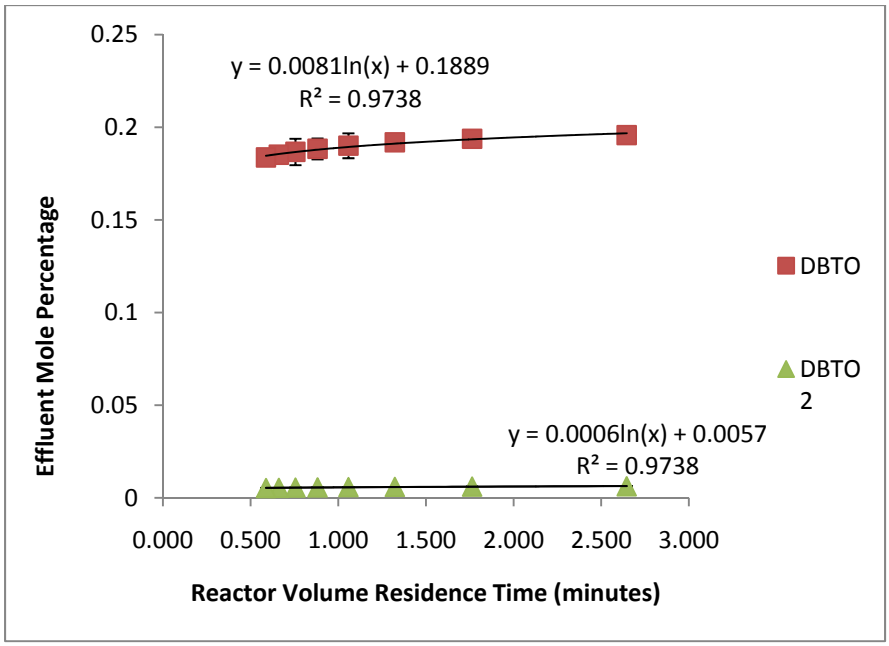


Figure 4.10 Effluent Mole Percentage of DBTO and $DBTO_2$ with 4:1 Flow Rate Ratio

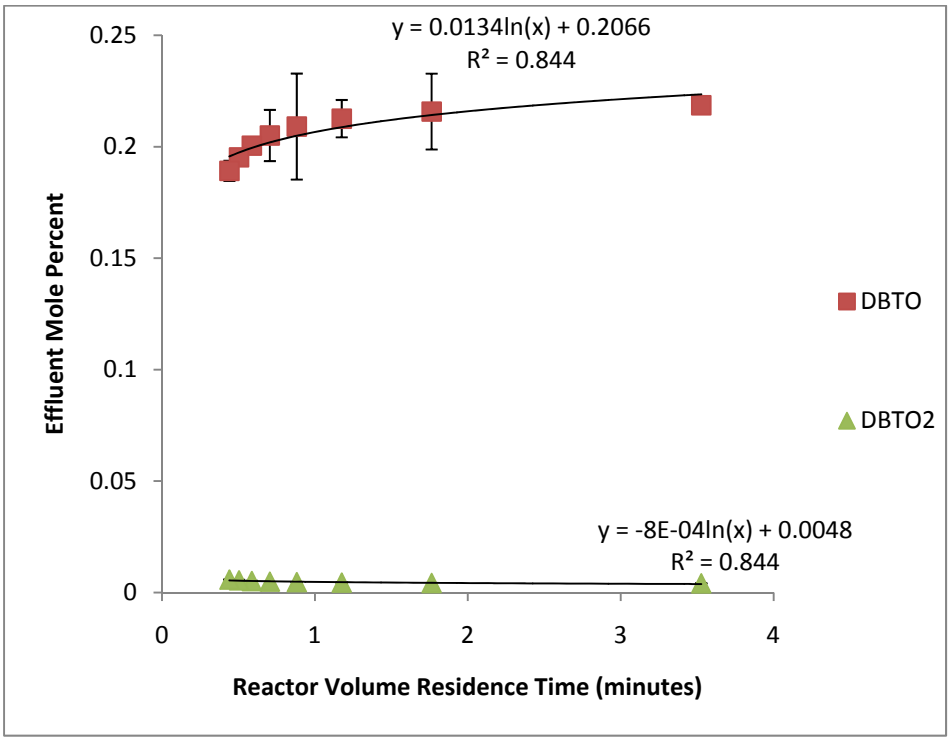


Figure 4.11 Effluent Mole Percentage of DBTO and $DBTO_2$ with 2:1 Flow Rate Ratio

These results of these three experiments show that an increase in the influent mole percentage of dibenzothiophene increases the production of DBTO while the production of $DBTO_2$ remains relatively constant throughout the experiment. The total conversion increases with an increase in the influent mole percentage of dibenzothiopene. For the 8:1, 4:1, and 2:1 experiments, the highest total conversion determined was 19.9%, 20.2%, and 22.3%. These results suggest that a smaller ratio of peroxide to DBT is condusive to the production of the second oxide.

The final component studied using this reactor type was the effect of reactor volume residence time at flow rate ratios (8:1, 4:1, and 2:1). The results of these three experiments follow the logical progression that longer residence time will lead to higher oxidation. All three experiments show either an increase in conversion across the residence time with the exception of DBTO in the 8:1 experiment and $DBTO_2$ in the 2:1 experiment, which both show very slightly negative trends as residence time increases. This may be due random error, as the slopes of the lines of best fit are orders of magnitude smaller than the trends found within this experiment. For example, the slope of the line of best fit for DBTO in the 8:1 experiment is -.002, while the slope for DBTO in the 2:1 experiment is .013, nearly an order of magnitude in difference. The small effluent mole percent of $DBTO_2$ is similar to the results of the highly concentrated peroxide experiment and further disproves the initial thought that more peroxide would ultimately lead to more oxidized product.

## 4.7 Peroxide Degradation

As a final test of the developed reactor, the degradation of the *tert*-butyl peroxide was tested. A new stock solution of equal strength of the previous was made. The 2:1 peroxide to dibenzothiophene flow rate ratio experiment was performed using this fresh peroxide solution to compare its strength against the previous solution,

which had been in use and storage for a much longer period of time. Figure 4.12 shows the results of this experiment.

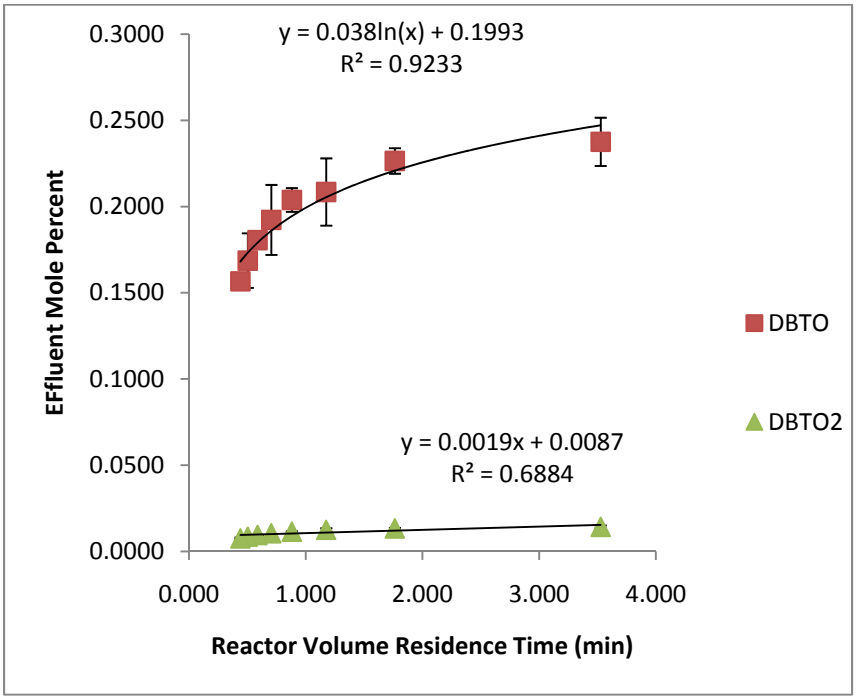


Figure 4.12 Effluent Mole Percentage of DBTO and $DBTO_2$ with 2:1 Flow Rate Ratio and Fresh Peroxide

In comparing this figure to its respective counterpart in Figure 4.11, it can be seen that the conversion of both DBTO and $DBTO_2$ increases dramatically. The degradation of the *tert*-butyl peroxide was to be expected due to its reactive nature. The fresh peroxide displayed much more conversion as it had not been given the opportunity to degrade. This suggests that the oxidant stream will need to be made with fresh chemicals in order to maintain a level of consistency within the reaction.

However, accounting for this phenomenon will make accurate modeling within the reaction volume slightly more difficult, but achievable if the entire reaction system (reaction volume, pre- and post-reaction volume, and age of chemicals) is taken into account. This would require modeling of the peroxide degradation over time, maintenance of the freshness of the chemicals and ensuring the no outside radicalization sources (i.e. light) are introduced to the system at any point.

# CHAPTER 5

# CONCLUSIONS AND RECOMMENDATIONS

## 5.1 Conclusions

A corona activated microreactor was designed, assembled and tested through the oxidative reaction of dibenzothiophene to its oxides by tert-butyl peroxide. This reaction may be useful as a model for the deep desulphurization of logistic fuels. The numbering up of this corona discharge activated microreactor system may be simpler and more straightforward than the numbering up of photochemical and other oxidative microreactor systems.

Several methods were explored in developing the method for which the corona could be developed, including testing a variety of materials for the proposed electrodes and electrode spacer. The strategy of combining a carbon nanotube based emitter electrode with a small gap between the emitter and collector electrodes as successful in giving a low turn on voltage for the microreactor.

Testing the reactor performance under a wide spread of conditions, including varying concentrations of dibenzothiophene, tert-butyl peroxide, reactor current, and reactor residence time allowed preliminary characterization of the reactor performance and capabilities. As expected, the higher current density leads to a

higher conversion of DBT to DBTO and $DBTO_2$. Higher concentrations of DBT in the fuel stream will lead to a higher conversion to DBTO but will inhibit the second oxidation to $DBTO_2$. However, at low initial DBT concentrations, high conversion to the $DBTO_2$ end product was observed suggesting that increasing conversion to the second oxide may be accomplished by increasing the charge dosage to the reacting fluid volume. We postulate that the clearly different device performance when compared to a photochemically activated reactor is due to a reaction mechanism where the DBT is radicalized or activated by the corona discharge to react with the oxidant source rather than the generally accepted photochemical activation step in which the oxidant source is cleaved by the radiation to generate reactive free radicals. It was determined that this reaction system is fully capable of activating the oxidative chemical reaction of DBT to its subsequent oxides under the presence of electrical energy and an oxidant source.

Of the experiments performed, one of the more peculiar results was that of the oxidation with no peroxide present. Mass balance calculations show that dissolved oxygen plays a role in the oxidative process. Indeed, a conversion of 10% and 36.5% for DBTO and $DBTO_2$ can be attributed to dissolved oxygen in decane. It follows in the next experiment, in which 550 PPM TBP is introduced into the system, that the mass balance predicts that dissolved oxygen continues to play a role in the oxidation.

## 5.2 Recommendations

This work has demonstrated the feasibility of activating chemicals reactions in microreactors via corona discharge. However, this technology is still within its infancy and a considerable amount of work must be done in order to realize its full potential.

Optimization and full exploration of the variables involved is needed for the developed microreactor. Variables needing to be explored are the effects of temperature, increasing applied current, and the reactor volume thickness, as well as continuing to test the variables discussed in this work. Figures 5.1A and B display the need for optimization of variables, showing how a high conversion of $DBTO_2$ does not necessarily correspond to a high amount of $DBTO_2$ produced. Figures 5.1A show a very high conversion and high throughput of $DBTO_2$ for the experimental set. However in comparison to other experiments, the highest throughput (approximately $1.8*10^{-8}$ moles of $DBTO_2$) is, comparatively, not exceedingly high. This is because of the low amount of DBT present in the stream so the oxidation of a dilute stream has a more substantial impact on the effluent conversion.

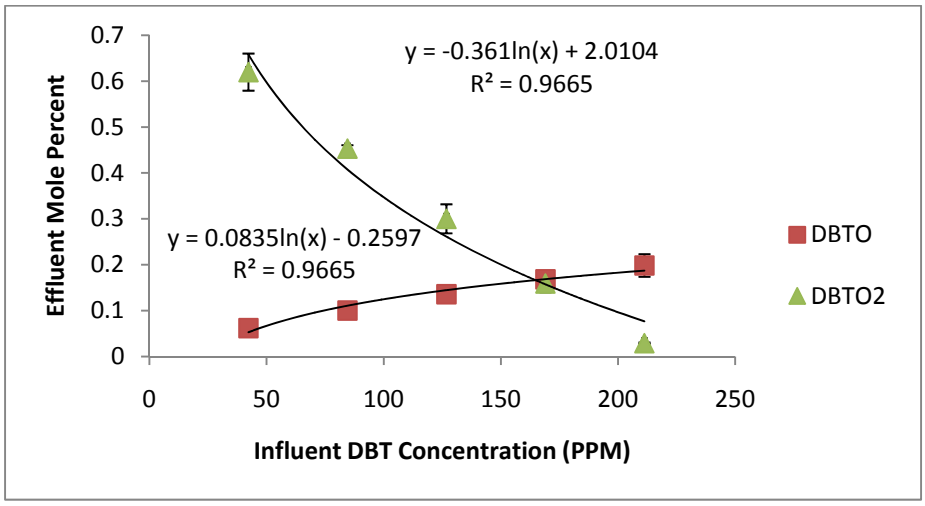


Figure 5.1A: Effluent Mole Percentage of DBTO and $DBTO_2$ for Highly Dilute Influent DBT Concentrations

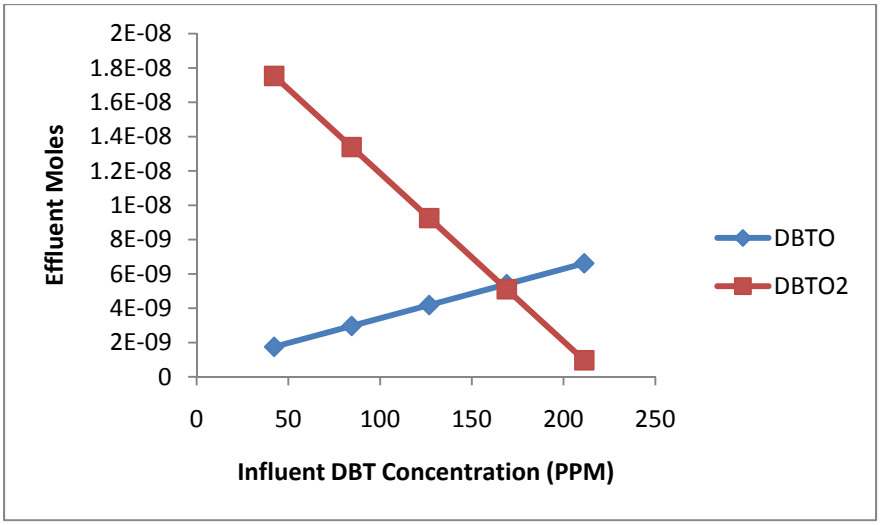


Figure 5.1B: Effluent Moles of DBTO and $DBTO_2$ for Highly Dilute Influent DBT Concentrations

In spite of the time spent developing this prototype reactor, several steps can be attempted to improve the efficiency and applicability of the reactor. First and foremost of these is the application of carbon nanotubes to the emitter electrode.

Currently, the nanotubes are randomly dispersed within silver epoxy. Through systematic and controlled growth of nanotube "forests," the current may become more evenly disbursed and conversion to oxidized species should increase.

Continuing along these lines, reactors must be made with a greater capability of reproducibility and possess the capability of disassembly without destruction. The current generation of reactors is permanently sealed and must be destroyed in order to investigate the interiors. A reactor that is not permanently sealed together but is capable of being sealed such that there are no leakages would be the goal of a second generation reactor. This work would include the aforementioned development of applying carbon nanotube forests, development on a more controlled application of a spacer between the electrodes via thin film deposition, and creation of microchannels for a more controlled, directional flow. Further work needs to be explored with regards to the ballast resistance and other methods capable of delivering higher amounts of current, voltage, and power to the reaction system to fully garner its capabilities.

Further into the research, industrial application should be discussed. This includes scaling up the microreactor to levels capable of continuous operation within a refinery. The scaling up process should include "numbering up" where the oil streams are sent through several microreactors in series and parallel to increase

volume of liquid reacted, decrease the conversion necessary by an individual reactor, and decrease overall cost associated with the process.

Another avenue that should be explored is the performance of a corona activated microreactor in a two phase or multiphase reacting system, such as in dual phase liquid reactors. For such a study, the organic, sulfur bearing stream would be mixed with an aqueous or polar steam that contains an oxidant source. The two would be sufficiently mixed and carried into the reactor system, similar to that described in this work. This combination may allow for simultaneous reaction and extraction of the oxidized sulfur bearing species from the organic fuel phase into the aqueous phase.

Literature has shown the level of removal of sulfur bearing species that commonly employed hydrodesulphurization is capable of. HDS is limited to removing easily reacted sulfur and nitrogen bearing compounds. Aromatic species, such as thiophene and its benzyl substituted derivates have been shown to be resistant to HDS and required other means of removal such as oxidative desulfurization. Literature has shown that the reactivity of the benzyl thiophene family decreases with the addition of a benzyl substituent or of a methyl group to the substituent. The reactivity decreases, respectively, from thiophene, benzothiophene, dibenzothiophene, 4-methyl dibenzothiophene, and 4,6-dimethyl dibenzothiophene.

In order to ensure this device is generally useful for oxidative desulphurization the oxidation of 4,6-dimethyl dibenzothiophene should be explored, as it is one of the more common, highly steric sulfur bearing species in fuels. In order to fully understand how this process must be applied in an industrial setting, a more realistic fuel source must be used. This should include, but not be limited to, varying grades of oil, several coexisting sulfur and nitrogen bearing species, and from different segments of the refining process to fully be able to optimize when and how this technology should be applied in an industrial setting.

Likewise, further study of the oxidant source should be included in future work in the specific application to oxidative desulphurization. Literature has shown several ODS applications using a wide range of oxygen sources including *tert*-butyl peroxide, *tert*-butyl hydroperoxide, hydrogen peroxide, other organic and inorganic peroxides, esters, ethers, organic acids, and dissolved oxygen. Of these, this work has shown that a very efficient method of oxidation is through the use of dissolved oxygen. This is a highly attractive option as it simplifies the oxidant addition to bubbling oxygen or air into the fuel stream.

In order to fully optimize the oxidant source, reactor specifications and industrial applications, modeling the kinetics of the oxidation reaction must be explored. Due to the unique nature of this reaction as compared to a UV-catalyzed ODS, the

reaction mechanism is unknown. Initially in this work, it was thought that the reaction would behave similarly to the reaction that was UV-catalyzed. However, this work has shown that an excess of the oxidative source did not necessarily lead to a higher conversion. In modeling the kinetics of this reaction, a great leap forward will be made in understanding the process as a whole and making headway towards its optimization.

Bibliography

1. "Diesel Education," http://www.sabertec.org/101_diesel Accessed July 30, 2010

2. "Ultra Low Sulfur Diesel Fuel: Summary Results of ULSD Quality and Availability," http://www.epa.gov/compliance/civil/caa/ultralow-sulfurdieselfuel.html Accessed July 30, 2010

3. Sugimoto, Y.; Aihara, Y.; Matsumura, A.; Ohi, A.; Sato, S.; Saito, I.; Yui, S., Processing of Middle East crude with Canadian oil sands bitumen-derived synthetic crude oil. *Journal of the Japan Petroleum Institute* **2006,** *49* (1), 1-12.

4. Okamoto, H.; Ushijima, T.; Kitoh, O., New methods for increasing productivity by using microreactors of planar pumping and alternating pumping types. *Chemical Engineering Journal* **2004,** *101* (1-3), 57-63.

5. Worz, O.; Jackel, K. P.; Richter, T.; Wolf, A., Microreactors, a new efficient tool for optimum reactor design. *Chemical Engineering Science* **2001,** *56* (3), 1029-1033.

6. Ma, X. L.; Sakanishi, K. Y.; Mochida, I., Hydrodesulfurization reactivities of various sulfur0compounds in diesel fuel. *Industrial & Engineering Chemistry Research* **1994,** *33* (2), 218-222.

7. Song, C.; Ma, X. L., New design approaches to ultra-clean diesel fuels by deep desulfurization and deep dearomatization. *Applied Catalysis B-Environmental* **2003,** *41* (1-2), 207-238.

8. "Low Sulfur Diesel," http://www.refineryscience.com/page131.htm , Accessed July 30, 2010

9. Houalla, M.; Broderick, D. H.; Sapre, A. V.; Nag, N. K.; Beer, V.; Gates, B. C.; Kwart, H., Hydrodesulfurization of methyl-substituted dibenzothiopehes catalyzed by sulfide CO-MO-Gamma-Al2O3. *Journal of Catalysis* **1980,** *61* (2), 523-527.

10. Nag, N. K.; Sapre, A. V.; Broderick, D. H.; Gates, B. C., Hydrodesulfurization of polycyclic aromatics catalyzed by sulfide COO-MOO3-Gamma-Al2O3 – Relative Reactivities. *Journal of Catalysis* **1979,** *57* (3), 509-512.

11. Torres-Nieto, J; Arevalo, A; Garcia, JJ; Catalytic Desulfurization of Dibenzothiophenes with Palladium Nanoparticles. *Inorganic Chemistry*. **2008** *47* (23), 11429-11434

12. Torres-Nieto, J; Arevalo, A; Garcia, JJ; Catalytic Desulfurization of Debenzothiopene and its hindered analogues with nickel and platinum compounds. *Organometallics.* **2007** *26* (9), 2228-2233

13. Al-Shahrani, F.; Xiao, T. C.; Llewellyn, S. A.; Barri, S.; Jiang, Z.; Shi, H. H.; Martinie, G.; Green, M. L. H., Desulfurization of diesel via the H2O2 oxidation of aromatic sulfides to sulfones using a tungstate catalyst. *Applied Catalysis B-Environmental* **2007,** *73* (3-4), 311-316.

14. Ramirez-Verduzco, L. F.; Reyes, J. A. D.; Torres-Garcia, E., Solvent effect in homogeneous and heterogeneous reactions to remove dibenzothiophene by an oxidation-extraction scheme. *Industrial & Engineering Chemistry Research* **2008,** *47* (15), 5353-5361.

15. Zapata, B.; Pedraza, F.; Valenzuela, M. A., Catalyst screening for oxidative desulfurization using hydrogen peroxide. *Catalysis Today* **2005,** *106* (1-4), 219-221.

16. Ali, S. H.; Hamad, D. M.; Albusairi, B. H.; Fahim, M. A., Removal of Dibenzothiophenes from Fuels by Oxy-desulfurization. *Energy & Fuels* **2009,** *23*, 5986-5994.

17. Campos-Martin, J. M.; Capel-Sanchez, M. C.; Fierro, J. L. G., Highly efficient deep desulfurization of fuels by chemical oxidation. *Green Chemistry* **2004,** *6* (11), 557-562.

18. Ukkirapandian, V.; Sadasivam, V.; Sivasankar, B., Oxidation of dibenzothiophene and desulphurization of diesel. *Petroleum Science and Technology* **2008,** *26* (4), 423-435.

19. Yu, G. X.; Lu, S. X.; Chen, H.; Zhu, Z. N., Diesel fuel desulfurization with hydrogen peroxide promoted by formic acid and catalyzed by activated carbon. *Carbon* **2005,** *43* (11), 2285-2294.

20. Shiraishi, Y.; Hara, H.; Hirai, T.; Komasawa, I., A deep desulfurization process for light oil by photosensitized oxidation using a triplet photosensitizer and hydrogen peroxide in an oil/water two-phase liquid-liquid extraction system. *Industrial & Engineering Chemistry Research* **1999,** *38* (4), 1589-1595.

21. Zhang, G. F.; Wang, R.; Yu, F. L.; Zhao, H. X., Clean fuel-oriented investigation of thiophene oxidation by hydrogen peroxide using polyoxometalate as catalyst. *Chemical Papers* **2009,** *63* (5), 617-619.

22. Lu, H. Y.; Gao, J. B.; Jiang, Z. X.; Yang, Y. X.; Song, B.; Li, C., Oxidative desulfurization of dibenzothiophene with molecular oxygen using emulsion catalysis. *Chemical Communications* **2007,** (2), 150-152.

23. Madeira, L. D.; Ferreira-Leitao, V. S.; Bon, E. P. D., Dibenzothiophene oxidation by horseradish peroxidase in organic media: Effect of the DBT : H2O2 molar ratio and H2O2 addition mode. *Chemosphere* **2008,** *71* (1), 189-194.

24. Chica, A.; Corma, A.; Domine, M. E., Catalytic oxidative desulfurization (ODS) of diesel fuel on a continuous fixed-bed reactor. *Journal of Catalysis* **2006,** *242* (2), 299-308.

25. Wang, D. H.; Qian, E. W. H.; Amano, H.; Okata, K.; Ishihara, A.; Kabe, T., Oxidative desulfurization of fuel oil - Part I. Oxidation of dibenzothiophenes using tert-butyl hydroperoxide. *Applied Catalysis a-General* **2003,** *253* (1), 91-99.

26. Ryu, K.; Kim, J.; Heo, J.; Chae, Y., Oxidation of dibenzothiophene catalyzed by immobilized hemoproteins in water-immiscible organic solvents. *Biotechnology Letters* **2002,** *24* (19), 1535-1538.

27. Grossman, M. J.; Lee, M. K.; Prince, R. C.; Minak-Bernero, V.; George, G. N.; Pickering, I. J., Deep desulfurization of extensively hydrodesulfurized middle distillate oil by Rhodococcus sp strain ECRD-1. *Applied and Environmental Microbiology* **2001,** *67* (4), 1949-1952.

28. Rhee, S. K.; Chang, J. H.; Chang, Y. K.; Chang, H. N., Desulfurization of dibenzothiophene and diesel oils by a newly isolated Gordona strain, CYKS1. *Applied and Environmental Microbiology* **1998,** *64* (6), 2327-2331.

29. Herbert, E.; Oxidative Desulfurization of Dibenzothiophene with Tert-Butyl Hydro Peroxide in a Photochemical Micro-Reactor. Oregon State University Thesis. **2007**

30. Matsuzawa, S.; Tanaka, J.; Sato, S.; Ibusuki, T., Photocatalytic oxidation of dibenzothiophenes in acetonitrile using TiO2: effect of hydrogen peroxide and

ultrasound irradiation. *Journal of Photochemistry and Photobiology a-Chemistry* **2002,** *149* (1-3), 183-189.

31. Zhang, J.; Zhao, D. S.; Yang, L. Y.; Li, Y. B., Photocatalytic oxidation dibenzothiophene using TS-1. *Chemical Engineering Journal* **2010,** *156* (3), 528-531.

32. Che, Y. K.; Ma, M. H.; Ji, H. W.; Zhao, J. C.; Zang, L., Visible photooxidation of dibenzothiophenes sensitized by 2-(4-methoxyphenyl)-4, 6-diphenylpyrylium: An electron transfer mechanism without involvement of superoxide. *Journal of Physical Chemistry B* **2006,** *110* (6), 2942-2948.

33. Wang, J. L.; Zhao, D. S.; Li, K. X., Oxidative Desulfurization of Dibenzothiophene Using Ozone and Hydrogen Peroxide in Ionic Liquid. *Energy & Fuels* **2010,** *24*, 2527-2529.

34. Castillo, K.; Parsons, J. G.; Chavez, D.; Chianelli, R. R., Oxidation of dibenzothiophene to dibenzothiophene-sulfone using silica gel. *Journal of Catalysis* **2009,** *268* (2), 329-334.

35. Lukes, P.; Locke, B. R., Plasmachemical oxidation processes in a hybrid gas-liquid electrical discharge reactor. *Journal of Physics D-Applied Physics* **2005,** *38* (22), 4074-4081.

36. Schiorlin, M.; Marotta, E.; Rea, M.; Paradisi, C., Comparison of Toluene Removal in Air at Atmospheric Conditions by Different Corona Discharges. *Environmental Science & Technology* **2009,** *43* (24), 9386-9392.

37. Kirkpatrick, M. J.; Finney, W. C.; Locke, B. R., Chlorinated organic compound removal by gas phase pulsed streamer corona electrical discharge with reticulated vitreous carbon electrodes. *Plasmas and Polymers* **2003,** *8* (3), 165-177.

38. Li, M. W.; Xu, G. H.; Tian, Y. L.; Chen, L.; Fu, H. F., Carbon dioxide reforming of methane using DC corona discharge plasma reaction. *Journal of Physical Chemistry A* **2004,** *108* (10), 1687-1693.

39. Sugiarto, A. T.; Ohshima, T.; Sato, M., Advanced oxidation processes using pulsed streamer corona discharge in water. *Thin Solid Films* **2002,** *407* (1-2), 174-178.

40. Mededovic, S.; Locke, B. R., Platinum catalysed decomposition of hydrogen peroxide in aqueous-phase pulsed corona electrical discharge. *Applied Catalysis B-Environmental* **2006,** *67* (3-4), 149-159.

41. Sahni, M.; Locke, B. R., Degradation of chemical warfare agent simulants using gas-liquid pulsed streamer discharges. *Journal of Hazardous Materials* **2006,** *137* (2), 1025-1034.

42. Collins, P. G.; Zettl, A., A simple and robust electron beam source from carbon nanotubes. *Applied Physics Letters* **1996,** *69* (13), 1969-1971.

43. de Jonge, N.; Lamy, Y.; Schoots, K.; Oosterkamp, T. H., High brightness electron beam from a multi-walled carbon nanotube. *Nature* **2002,** *420* (6914), 393-395.

44. Kang, Y.; Wu, Z. C., Formation of hydroxyl radicals and oxidation of toluene under corona discharge with water vapor as radical source. *Chinese Science Bulletin* **2008,** *53* (14), 2248-2252.

45. Lock, E. H.; Saveliev, A. V.; Kennedy, L. A., Methanol and dimethyl sulfide removal by pulsed corona part I: Experiment. *Plasma Chemistry and Plasma Processing* **2006,** *26* (6), 527-542.

46. Magne, L.; Blin-Simiand, N.; Gadonna, K.; Jeanney, P.; Jorand, F.; Pasquiers, S.; Postel, C., OH kinetics in photo-triggered discharges used for VOCs conversion. *European Physical Journal-Applied Physics* **2009,** *47* (2), 9.

47. Marotta, E.; Callea, A.; Rea, M.; Paradisi, C., DC corona electric discharges for air pollution control. Part 1. Efficiency and products of hydrocarbon processing. *Environmental Science & Technology* **2007,** *41* (16), 5862-5868.

48. Locke, B. R.; Sato, M.; Sunka, P.; Hoffmann, M. R.; Chang, J. S., Electrohydraulic discharge and nonthermal plasma for water treatment. *Industrial & Engineering Chemistry Research* **2006,** *45* (3), 882-905.

49. Sharma, A. K.; Josephson, G. B.; Camaioni, D. M.; Goheen, S. C., Destruction of pentachlorophenol using glow discharge plasma process. *Environmental Science & Technology* **2000,** *34* (11), 2267-2272.

50. Sugiarto, A. T.; Sato, M., Pulsed plasma processing of organic compounds in aqueous solution. *Thin Solid Films* **2001,** *386* (2), 295-299.

# APPENDICES

Appendix A. Literature Review Summary

The following table presents previously published information regarding desulfurization systems.

Table A.1. Summary of Desulfurization Methods

| Reference | Sulfur Compounds | Oxidant | Catalyst | Solvent | Type |
|---|---|---|---|---|---|
| Al-Shanhrani, et. al., 2007 | DBT, 4,6-DMDBT | $H_2O_2$ | $Na_2WO_4$ | Methanol | Dual Phase |
| Ali, et. al., 2009 | DBT | $H_2O_2$ | Acetic Acid | NMP, DMF, ACN | Dual Phase |
| Campos-Martin, et.al., 2004 | BT, DBT, EMDBT | $H_2O_2$ | $H_2WO_4$ | ACN | Dual Phase |
| Castillo, et.al., 2009 | DBT | -- | $SiO_2$ | Decalin, Tetralin, Heptane, Toluene, Dodecane | Misc. |
| Che, et.al., 2006 | DBT | $O_2$ | $MOPDPP^+BF_4^-$ | ACN | Misc. |
| Chica, et.al., 2006 | T, BT, 2-MT, 2-MBT, DBT, 4-MDBT, 4,6-DMDBT | TBHP | Ti-MCM-42, MoOx/AL2O3 | -- | Single Phase |
| Grossman, et.al., 2001 | DBT, 4,6-DMDBT | -- | *Rhodococcus* sp. Strain ECRD-1 | Methylene Chloride | Biological |
| Lu, et.al., 2006 | DBT | $O_2$ | Polyoxometalate anion | Acetonitrile | Dual Phase |
| Madeira, et.al., 2008 | DBT | $H_2O_2$ | Horseradish Peroxidase | Acetonitrile | Dual Phase |
| Matsuzawa, et.al., 2002 | DBT, 4,6-DMDBT | $H_2O_2$ | $TiO_2$ | -- | Misc. |
| Ramirez-Verduzco, et.al., 2008 | DBT | $H_2O_2$ | $WO_x$-$ZrO_2$ | Methanol, ethanol, acetonitrile, γ-butyrolactone | Dual Phase |
| Rhee, et.al., 1998 | DBT | -- | *Gordona* Strain, CYKS1 | -- | Biological |
| Ryu., et.al., 2002 | DBT | $H_2O_2$, TBHP, α, α-dimethylbenzyl hydroperoxide | Hemoglobin, Myoglobin, Cytochrome c | -- | Single Phase |
| Shiraishi, et.al., 1999 | DBT | $H_2O_2$ | Benzophenone | Water | Dual Phase |
| Ukkirapandian, et.al., 2008 | DBT | $H_2O_2$ | Acids | Water | Dual Phase |
| Wang, et.al., 2003 | BT, DBT, 4-MDBT, 4,6-DMDBT | TBHP | Mo, Cr, W, V, Nb, Zr based | -- | Single Phase |
| Wang J., et.al., 2010 | DBT | Ozone, $H_2O_2$ | Ionic Liquids | Ionic Liquids | Misc. |
| Yu, et.al., 2005 | DBT | $H_2O_2$ | Formic Acid, Activated Carbon | Water | Dual Phase |
| Zapata, et.al., 2005 | T, BT, DBT | $H_2O_2$ | Pd, $Cr_2O_3$, $MnO_x$, Co-Mo/$Al_2O_3$ | Hexadecane, ACN | Dual Phase |
| Zhang, et.al., 2009 | T | $H_2O_2$ | Polyoxometalates | -- | Dual Phase |
| Zhang, et.al., 2010 | DBT | $H_2O_2$ | TS-1 | -- | Misc. |

The following table shows previously published information on corona discharge plasma, including the literature source, discharge source, phase in which the discharge occurs, radical source, and the targeted chemical.

A.2. Summary of Corona Discharge Methods

| Reference | Discharge Source | Discharge Phase | Radical Source | Targeted Chemical |
|---|---|---|---|---|
| Collins, et.al., 1996 | CNT | -- | -- | -- |
| de Jonge, et.al. 2002 | CNT | -- | -- | -- |
| Kang, et.al. 2008 | -- | Gas (air) | Water | Toluene |
| Kirkpatrick, et.al. 2003 | Platinum-rhodium | Gas | Water | TCE, VC |
| Li, et.al., 2004 | Stainless Steel | Gas | $CO_2$ | $CH_4$, $CO_2$ |
| Lock, et.al., 2006 | -- | Gas | Water | Methanol, Dimethyl Suflide |
| Locke, et.al., 2006 | -- | Liquid, Gas, Liquid/Gas interface | Water | Pollutants in Water Treatment |
| Lukes, et.al., 2005 | -- | Liquid, Gas | $O_2$, Ar, Water | Phenol |
| Magne, et.al., 2009 | -- | Gas | $O_2$, Water | Acetone, IPA |
| Marotta, et.al., 2007 | Stainless Steel | Gas | $O_2$, n-hexane, i-octante | n-hexane, i-octane |
| Mededovic, et.al., 2006 | NiCr, Pt | Liquid | $H_2O_2$ | -- |
| Sahni, et.al., 2006 | NiCr | Liquid | $H_2O_2$ | Ferrous Sulfate, G agent stimulant |
| Schiorlin, et. al., 2009 | Stainless Steel | Gas | $O_2$ | Toluene |
| Sharma, et.al., 2000 | Stainless Steel | Gas/Liquid | Water | PCP |
| Shih, et.al., 2009 | NiCr | Gas in Liquid | $H_2$, $H_2O_2$ | $H_2$, $H_2O_2$ |
| Sugiarto, et.al., 2001 | Stainless Steel | Liquid | $O_2$ (gas) | Phenol |
| Sugiarto, et.al., 2002 | Stainless Steel (ring) | Liquid | $H_2O_2$ | Organic Dyes |

Appendix B: Reactor Specs Calculations

Inner diameter of PEEK tubing: 508 microns (.000508 m)

Cross sectional Area of PEEK tubing: $8.10732*10^{-7}$ $m^2$

| Total Flow Rate (µL/min) | Flow Rate ($m^3$/min) | Velocity (m/min) | Tube Length (m) | Residence Time (minutes) |
|---|---|---|---|---|
| 100 | $1*10^{-7}$ | .12334 | 1 | 8.1073 |
| 100 | $1*10^{-7}$ | .12334 | .7 | 5.6751 |
| 100 | $1*10^{-7}$ | .12334 | .5 | 4.0536 |
| 100 | $1*10^{-7}$ | .12334 | .3 | 2.4322 |
| 100 | $1*10^{-7}$ | .12334 | .2 | 1.6214 |
| 100 | $1*10^{-7}$ | .12334 | .1 | .81073 |

Plotting the tube length against the residence time gives a direct relationship between the two as follows:

$$\boldsymbol{Tube\ Residence\ Time\ (minutes) = 8.1073 * Tube\ length\ (m)}$$

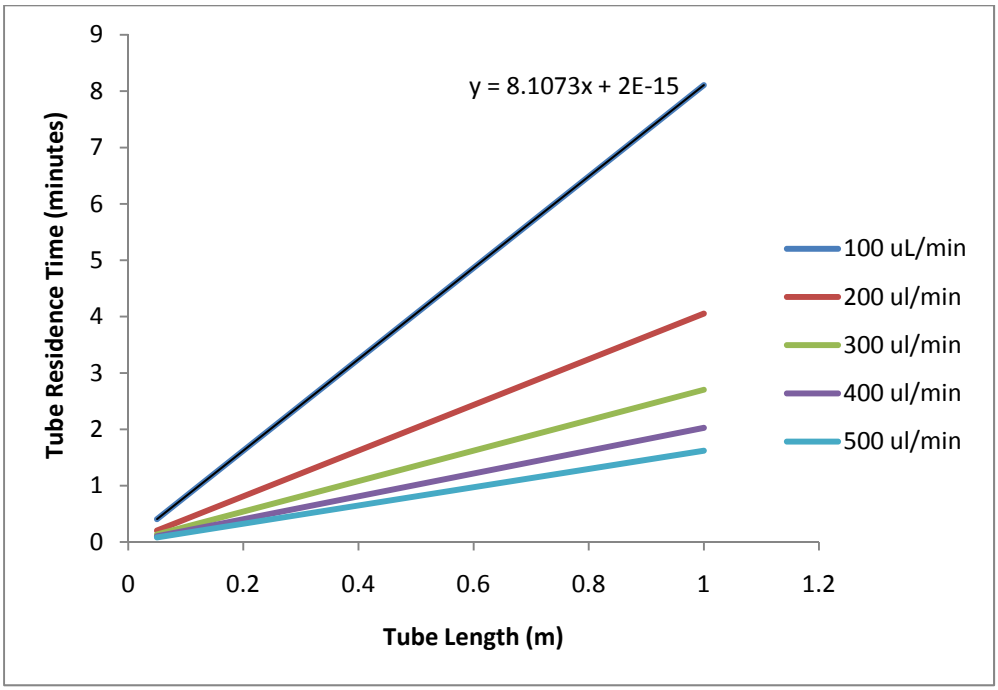


Figure B.1: Plot of tube length and tube residence times at multiple flow rates

The specifics of the reactor size and experimental time were determined by the following protocol:

1. Allow the reactor system (comprised of tubes from syringe pump tube from micromixer to reactor, reactor volume, and effluent tube) to dry completely
2. Turn on syringe pump to a predetermined flow rate and start timer
3. Measure the length of time until the first drop leaves the effluent tubes

The following data was determined though direct measurement:

- Inlet tube length: 25 cm (.25 m)
- Outlet tube length: 40 cm (.40 m)
- Total residence time: 7 minutes 54.9 seconds (7.915 minutes)
- Cross sectional area of PEEK tubing: $8.10732*10^{-7}$ $m^2$
- Relationship between tube length and tube residence time
  - Shown above
- Flow Rate: 100 µL/min ($1*10^{-7}$ $m^3$/min)
- Reactor Volume length = 5 cm
- Reactor Volume Width = 2 cm
- Reactor Volume Area = 10 $cm^2$

The following data is determined through manipulation of the above data:

Inlet Tube

$$.25\ \boldsymbol{m} * 8.1073 = 2.0268\ \boldsymbol{minutes}\ (\boldsymbol{residence\ time})$$

$$2.0268\ \boldsymbol{minutes} * 1 * 10^{-7}\frac{\boldsymbol{m^3}}{\boldsymbol{minute}} = 2.02683 * 10^{-7}\ \boldsymbol{m^3}\ * \left(100\frac{\boldsymbol{cm}}{\boldsymbol{m}}\right)^3$$
$$=.20268\ \boldsymbol{cm^3}\ (\boldsymbol{volume})$$

Outlet Tube

$$.40\ \boldsymbol{m} * 8.1073 = 3.24292\ \boldsymbol{minutes}\ (\boldsymbol{residence\ time})$$

$$3.24292\ \boldsymbol{minutes} * 1 * 10^{-7}\frac{\boldsymbol{m^3}}{\boldsymbol{minute}} = 3.24292 * 10^{-7}\ \boldsymbol{m^3} * \left(100\frac{\boldsymbol{cm}}{\boldsymbol{m}}\right)^3$$
$$=.324295\ \boldsymbol{cm^3}\ (\boldsymbol{volume})$$

Total System

$$\mathbf{7.915\ minutes} * \mathbf{1} * \mathbf{10^{-7}}\ \frac{\boldsymbol{m^3}}{\boldsymbol{minute}} = \mathbf{7.915} * \mathbf{10^{-7}}\ \boldsymbol{m^3} * \left(\mathbf{100}\ \frac{\boldsymbol{cm}}{\boldsymbol{m}}\right)^{\mathbf{3}}$$
$$= .\mathbf{7915}\ \boldsymbol{cm^3}\ (\boldsymbol{total\ volume})$$

$$\boldsymbol{Total\ volume} = \boldsymbol{Inlet\ Tube\ Volume} + \boldsymbol{Outlet\ Tube\ Volume} + \boldsymbol{Reactor\ Volume}$$

Reactor Volume/Height

$$.\mathbf{7915}\ \boldsymbol{cm^3} - .\mathbf{324295}\ \boldsymbol{cm^3} - .\mathbf{20268}\ \boldsymbol{cm^3} = .\mathbf{26452}\ \boldsymbol{cm^3}$$

$$\frac{(.\mathbf{26452}\ cm^3)}{10\ cm^2} = .026452\ cm\ *\ 10^4\ \frac{\mu m}{cm} = 264.5\ \mu m\ (control\ volume\ height)$$

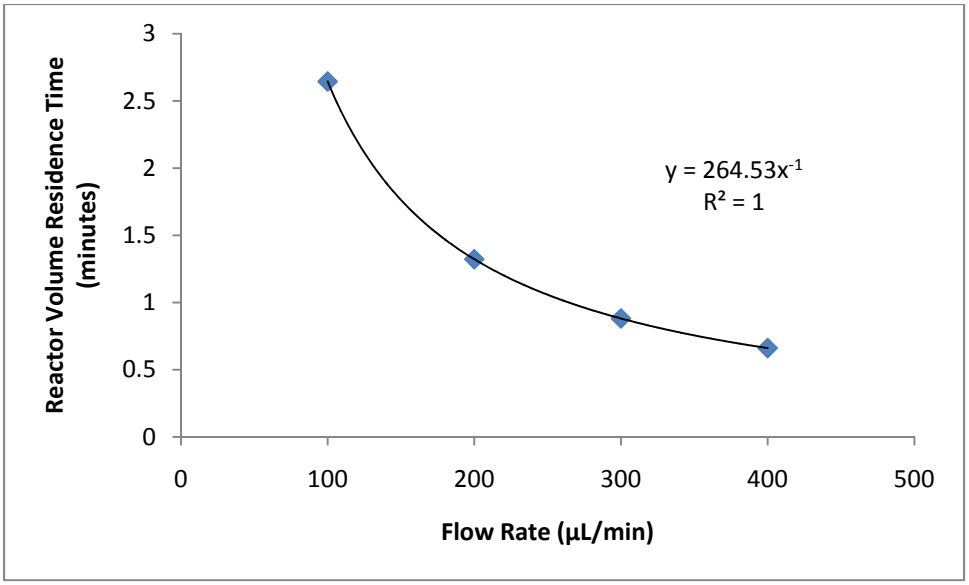


Figure B.2: Relationship between total influent flow rate and reactor volume residence time

# Appendix C: Protocols

## C.1 Experiment 1

1. Load both syringes with the standard solutions of dibenzothiophene and peroxide
2. Mount syringes into pumps and attach tubing.
3. Set both pumps to 100 µL/min and turn on
4. Allow first drop to leave effluent tube
5. Turn on Power Supply and select “Integrate”
6. Set the Voltage to 50 V, Current to 20 mA, and Power to 20 W
7. Based off of Appendix A, determine total residence time for system
8. Wait for system to equilibrate for 3x total residence time
9. Collect 3 samples in 2 mL vials and cap
10. Stop syringe pumps and power supply
11. Change voltage to 60 V

    (70,80,90,100,110,120,130,140,150,160,170,180,190,200,300,400,500,600,700,800,

    900,1000,1100,1200,1300,1400,1500 V)
12. Repeat steps 6-13 until total flow rate (dibenzothiophene + peroxide) is 600 µL/min
13. Store samples at -10°C until ready for analytical testing

C.2 Experiment 2

1. Prepare dilutions of dibenzothiophene by measuring out .5, 1, 2, 3, 4, 5, 6, 7, 8, and 9 milliliters of the standard 4226 PPM solution and adding the subsequent amount of decane necessary to bring the total volume to 10 milliliters.
2. Load the smallest concentration (.5 milliliter solution) into dibenzothiophene syringe and standard peroxide into peroxide syringe.
3. Mount syringes into pumps and attach tubing.
4. Set flow rates to 100 µL/min and turn on pumps.
5. Allow first drop to leave effluent tube
6. Turn on Power Supply and select “Integrate”
7. Set the Voltage to 500 V, Current to 20 mA, and Power to 20 W
8. Based off of Appendix A, determine total residence time for system
9. Wait for system to equilibrate for 3x total residence time
10. Collect 3 samples in 2 mL vials and cap
11. Stop syringe pumps and power supply
12. Empty dibenzothiophene syringe into waste and clean out with pure decane
13. Add next smallest concentration of dibenzothiophene
14. Repeat steps 3-13 until all concentrations have been run
15. Store samples at -10°C until ready for analytical testing

C.3 Experiment 3

1. Prepare dilutions of dibenzothiophene by measuring out .1, .2, .3, .4, and .5 milliliters of the standard 4226 PPM solution and adding the subsequent amount of decane necessary to bring the total volume to 10 milliliters.
2. Load the smallest concentration (.1 milliliter solution) into dibenzothiophene syringe and standard peroxide into peroxide syringe.
3. Mount syringes into pumps and attach tubing.
4. Set flow rates to 100 µL/min and turn on pumps.
5. Allow first drop to leave effluent tube
6. Turn on Power Supply and select “Integrate”
7. Set the Voltage to 500 V, Current to 20 mA, and Power to 20 W
8. Based off of Appendix A, determine total residence time for system
9. Wait for system to equilibrate for 3x total residence time
10. Collect 3 samples in 2 mL vials and cap
11. Stop syringe pumps and power supply
12. Empty dibenzothiophene syringe into waste and clean out with pure decane
13. Add next smallest concentration of dibenzothiophene
14. Repeat steps 3-13 until all concentrations have been run
15. Store samples at -10°C until ready for analytical testing

C.4 Experiment 4

1. Prepare 20x standard solution (110300 PPM) of peroxide.
2. Measure out 1, 2, 3, 4, 5, 6, 7, 8, 9, and 0 milliliters of the 110300 PPM solution and adding the subsequent amount of decane necessary to bring the total volume to 10 milliliters.
3. Load the smallest concentration (1 milliliter solution) into peroxide syringe and standard dibenzothiophene into dibenzothiophene syringe.
4. Mount syringes into pumps and attach tubing.
5. Set flow rates to 100 µL/min and turn on pumps.
6. Allow first drop to leave effluent tube
7. Turn on Power Supply and select “Integrate”
8. Set the Voltage to 500 V, Current to 20 mA, and Power to 20 W
9. Based off of Appendix A, determine total residence time for system
10. Wait for system to equilibrate for 3x total residence time
11. Collect 3 samples in 2 mL vials and cap
12. Stop syringe pumps and power supply
13. Empty peroxide syringe into waste and clean out with pure decane
14. Add next smallest concentration of peroxide
15. Repeat steps 3-14 until all concentrations have been run
16. Store samples at -10°C until ready for analytical testing

C.5 Experiment 5

1. Measure out 0, 1, 2, 3, 4, 5, 6, and 7 milliliters of the standard 5515 PPM solution and adding the subsequent amount of decane necessary to bring the total volume to 10 milliliters.
2. Load the smallest concentration (0 milliliter solution) into peroxide syringe and standard dibenzothiophene into dibenzothiophene syringe.
3. Mount syringes into pumps and attach tubing.
4. Set flow rates to 100 µL/min and turn on pumps.
5. Allow first drop to leave effluent tube
6. Turn on Power Supply and select “Integrate”
7. Set the Voltage to 500 V, Current to 20 mA, and Power to 20 W
8. Based off of Appendix A, determine total residence time for system
9. Wait for system to equilibrate for 3x total residence time
10. Collect 3 samples in 2 mL vials and cap
11. Stop syringe pumps and power supply
12. Empty peroxide syringe into waste and clean out with pure decane
13. Add next smallest concentration of peroxide
14. Repeat steps 2-13 until all concentrations have been run
15. Store samples at -10°C until ready for analytical testing

C.6 Experiment 6

1. Load both syringes with the standard solutions of dibenzothiophene and peroxide
2. Mount syringes into pumps and attach tubing.
3. Set dibenzothiophene flow rates to 25 µL/min, peroxide flow rate to 50 µL/min and turn on pumps.
4. Allow first drop to leave effluent tube
5. Turn on Power Supply and select “Integrate”
6. Set the Voltage to 500 V, Current to 20 mA, and Power to 20 W
7. Based off of Appendix A, determine total residence time for system
8. Wait for system to equilibrate for 3x total residence time
9. Collect 3 samples in 2 mL vials and cap
10. Stop syringe pumps and power supply
11. Change flow rates of dibenzothiophene by 25 µL/min and of peroxide by 50 µL/min
12. Repeat steps 3-11 until total flow rate (dibenzothiophene + peroxide) is 600 µL/min
13. Store samples at -10°C until ready for analytical testing

C.7 Experiment 7

1. Load both syringes with the standard solutions of dibenzothiophene and peroxide
2. Mount syringes into pumps and attach tubing.
3. Set dibenzothiophene flow rates to 20 µL/min, peroxide flow rate to 80 µL/min and turn on pumps.
4. Allow first drop to leave effluent tube
5. Turn on Power Supply and select “Integrate”
6. Set the Voltage to 500 V, Current to 20 mA, and Power to 20 W
7. Based off of Appendix A, determine total residence time for system
8. Wait for system to equilibrate for 3x total residence time
9. Collect 3 samples in 2 mL vials and cap
10. Stop syringe pumps and power supply
11. Change flow rates of dibenzothiophene by 10 µL/min and of peroxide by 40 µL/min
12. Repeat steps 3-11 until total flow rate (dibenzothiophene + peroxide) is 450 µL/min
13. Store samples at -10°C until ready for analytical testing

C.8 Experiment 8

1. Load both syringes with the standard solutions of dibenzothiophene and peroxide
2. Mount syringes into pumps and attach tubing.
3. Set dibenzothiophene flow rates to 10 µL/min, peroxide flow rate to 80 µL/min and turn on pumps.
4. Allow first drop to leave effluent tube
5. Turn on Power Supply and select “Integrate”
6. Set the Voltage to 500 V, Current to 20 mA, and Power to 20 W
7. Based off of Appendix A, determine total residence time for system
8. Wait for system to equilibrate for 3x total residence time
9. Collect 3 samples in 2 mL vials and cap
10. Stop syringe pumps and power supply
11. Change flow rates of dibenzothiophene by 10 µL/min and of peroxide by 80 µL/min
12. Repeat steps 3-11 until total flow rate (dibenzothiophene + peroxide) is 630 µL/min
13. Store samples at -10°C until ready for analytical testing

C.9 Experiment 9

1. Load both syringes with the standard solutions of dibenzothiophene and peroxide
2. Mount syringes into pumps and attach tubing.
3. Attach 1 meter effluent tube to effluent hole, seal and dry
4. Set both pumps to 100 µL/min and turn on
5. Allow first drop to leave effluent tube
6. Turn on Power Supply and select “Integrate”
7. Set the Voltage to 50 V, Current to 20 mA, and Power to 20 W
8. Based off of Appendix A, determine total residence time for system
9. Wait for system to equilibrate for 3x total residence time
10. Collect 3 samples in 2 mL vials and cap
11. Stop syringe pumps and power supply
12. Clip end of effluent tube with wire cutters to .9 m (.8,.7,.6,.5,.4,.35,.3,.2,.15,.1,.05 m)
13. Repeat steps 4-12 until total flow rate (dibenzothiophene + peroxide) is 600 µL/min
14. Store samples at -10°C until ready for analytical testing

C.10 Experiment 10

1. Remade stock solution of peroxide with new peroxide that has not been exposed to light or given time to degrade
2. Load both syringes with the standard solutions of dibenzothiophene and new peroxide
3. Mount syringes into pumps and attach tubing.
4. Set dibenzothiophene flow rates to 25 µL/min, peroxide flow rate to 50 µL/min and turn on pumps.
5. Allow first drop to leave effluent tube
6. Turn on Power Supply and select “Integrate”
7. Set the Voltage to 500 V, Current to 20 mA, and Power to 20 W
8. Based off of Appendix A, determine total residence time for system
9. Wait for system to equilibrate for 3x total residence time
10. Collect 3 samples in 2 mL vials and cap
11. Stop syringe pumps and power supply
12. Change flow rates of dibenzothiophene by 25 µL/min and of peroxide by 50 µL/min
13. Repeat steps 3-11 until total flow rate (dibenzothiophene + peroxide) is 600 µL/min
14. Store samples at -10°C until ready for analytical testing

# Appendix D. Tabulated Results

## D.1. Current Data

| | Effluent Moles | | | Effluent Mole % | | |
|---|---|---|---|---|---|---|
| Current (mA) | DBT | DBTO | DBTO2 | DBT | DBTO | DBTO2 |
| 0.16 | 1.20E-07 | 2.75E-08 | 2.10E-08 | 0.7129 | 0.1628 | 0.1244 |
| 0.2 | 1.21E-07 | 2.78E-08 | 2.13E-08 | 0.7119 | 0.1630 | 0.1252 |
| 0.235 | 1.22E-07 | 2.81E-08 | 2.17E-08 | 0.7110 | 0.1631 | 0.1258 |
| 0.28 | 1.24E-07 | 2.85E-08 | 2.21E-08 | 0.7100 | 0.1633 | 0.1267 |
| 0.325 | 1.25E-07 | 2.88E-08 | 2.25E-08 | 0.7089 | 0.1635 | 0.1275 |
| 0.36 | 1.26E-07 | 2.91E-08 | 2.28E-08 | 0.7081 | 0.1637 | 0.1282 |
| 0.405 | 1.27E-07 | 2.95E-08 | 2.32E-08 | 0.7071 | 0.1639 | 0.1290 |
| 0.45 | 1.29E-07 | 2.99E-08 | 2.36E-08 | 0.7062 | 0.1641 | 0.1298 |
| 0.5 | 1.30E-07 | 3.03E-08 | 2.41E-08 | 0.7051 | 0.1643 | 0.1306 |
| 0.54 | 1.31E-07 | 3.06E-08 | 2.45E-08 | 0.7043 | 0.1644 | 0.1313 |
| 0.585 | 1.32E-07 | 3.10E-08 | 2.49E-08 | 0.7034 | 0.1646 | 0.1320 |
| 0.635 | 1.34E-07 | 3.14E-08 | 2.53E-08 | 0.7024 | 0.1648 | 0.1328 |
| 0.68 | 1.35E-07 | 3.18E-08 | 2.57E-08 | 0.7015 | 0.1650 | 0.1335 |
| 0.73 | 1.37E-07 | 3.22E-08 | 2.62E-08 | 0.7005 | 0.1652 | 0.1343 |
| 0.78 | 1.38E-07 | 3.26E-08 | 2.67E-08 | 0.6996 | 0.1654 | 0.1350 |
| 0.84 | 1.40E-07 | 3.31E-08 | 2.72E-08 | 0.6985 | 0.1656 | 0.1359 |
| 1.41 | 1.56E-07 | 3.79E-08 | 3.24E-08 | 0.6896 | 0.1673 | 0.1431 |
| 1.98 | 1.73E-07 | 4.27E-08 | 3.76E-08 | 0.6825 | 0.1687 | 0.1488 |
| 2.56 | 1.89E-07 | 4.75E-08 | 4.29E-08 | 0.6767 | 0.1699 | 0.1535 |
| 3.195 | 2.08E-07 | 5.28E-08 | 4.88E-08 | 0.6714 | 0.1709 | 0.1577 |
| 3.76 | 2.24E-07 | 5.76E-08 | 5.39E-08 | 0.6675 | 0.1716 | 0.1608 |
| 4.33 | 2.40E-07 | 6.23E-08 | 5.92E-08 | 0.6642 | 0.1723 | 0.1635 |
| 4.91 | 2.57E-07 | 6.72E-08 | 6.45E-08 | 0.6612 | 0.1729 | 0.1659 |
| 5.5 | 2.74E-07 | 7.21E-08 | 6.99E-08 | 0.6586 | 0.1734 | 0.1680 |
| 6.1 | 2.91E-07 | 7.71E-08 | 7.54E-08 | 0.6563 | 0.1738 | 0.1698 |
| 6.73 | 3.09E-07 | 8.24E-08 | 8.11E-08 | 0.6542 | 0.1742 | 0.1716 |
| 7.35 | 3.27E-07 | 8.76E-08 | 8.68E-08 | 0.6523 | 0.1746 | 0.1731 |
| 8 | 3.46E-07 | 9.30E-08 | 9.27E-08 | 0.6506 | 0.1750 | 0.1745 |
| 8.66 | 3.65E-07 | 9.85E-08 | 9.88E-08 | 0.6490 | 0.1753 | 0.1757 |

D.2. High DBT Concentration Data

| | Effluent Moles | | | Effluent Mole % | | |
|---|---|---|---|---|---|---|
| DBT Concentration (PPM) | DBT | DBTO | DBTO2 | DBT | DBTO | DBTO2 |
| 211.3 | 4.77E-09 | 3.08E-09 | 1.26E-09 | 0.5238 | 0.3382 | 0.1380 |
| 422.6 | 1.35E-08 | 5.21E-09 | 1.28E-09 | 0.6759 | 0.2603 | 0.0638 |
| 845.2 | 3.10E-08 | 9.47E-09 | 1.32E-09 | 0.7422 | 0.2264 | 0.0314 |
| 1267.8 | 4.86E-08 | 1.37E-08 | 1.35E-09 | 0.7630 | 0.2157 | 0.0213 |
| 1690.4 | 6.61E-08 | 1.80E-08 | 1.39E-09 | 0.7732 | 0.2105 | 0.0163 |
| 2113 | 8.36E-08 | 2.22E-08 | 1.43E-09 | 0.7793 | 0.2074 | 0.0133 |
| 2535.6 | 1.01E-07 | 2.65E-08 | 1.47E-09 | 0.7833 | 0.2053 | 0.0114 |
| 2958.2 | 1.19E-07 | 3.08E-08 | 1.51E-09 | 0.7862 | 0.2038 | 0.0100 |
| 3380.8 | 1.36E-07 | 3.50E-08 | 1.55E-09 | 0.7883 | 0.2028 | 0.0090 |
| 3803.4 | 1.54E-07 | 3.93E-08 | 1.59E-09 | 0.7899 | 0.2019 | 0.0082 |

D.3. Low DBT Concentration Data

| | Effluent Moles | | | Effluent Mole % | | |
|---|---|---|---|---|---|---|
| DBT Concentration (PPM) | DBT | DBTO | DBTO2 | DBT | DBTO | DBTO2 |
| 42.26 | 9.02E-09 | 1.75E-09 | 1.75E-08 | 0.3187 | 0.0617 | 0.6196 |
| 84.52 | 1.32E-08 | 2.96E-09 | 1.34E-08 | 0.4468 | 0.1002 | 0.4530 |
| 126.78 | 1.74E-08 | 4.18E-09 | 9.25E-09 | 0.5644 | 0.1356 | 0.3000 |
| 169.04 | 2.16E-08 | 5.4E-09 | 5.11E-09 | 0.6727 | 0.1682 | 0.1591 |
| 211.3 | 2.58E-08 | 6.62E-09 | 9.68E-10 | 0.7728 | 0.1982 | 0.0290 |

D.4. High Peroxide Concentration Data

| | Effluent Moles | | | Effluent Mole % | | |
|---|---|---|---|---|---|---|
| Peroxide Concentration (PPM) | DBT | DBTO | DBTO2 | DBT | DBTO | DBTO2 |
| 11030 | 1.07E-07 | 2.63E-08 | 1.07E-09 | 0.7967 | 0.1954 | 0.0079 |
| 22060 | 1.19E-07 | 2.93E-08 | 1.12E-09 | 0.7964 | 0.1961 | 0.0075 |
| 33090 | 1.31E-07 | 3.23E-08 | 1.18E-09 | 0.7961 | 0.1967 | 0.0072 |
| 44120 | 1.42E-07 | 3.52E-08 | 1.24E-09 | 0.7959 | 0.1972 | 0.0069 |
| 55150 | 1.54E-07 | 3.82E-08 | 1.29E-09 | 0.7957 | 0.1976 | 0.0067 |
| 66180 | 1.65E-07 | 4.12E-08 | 1.35E-09 | 0.7955 | 0.1980 | 0.0065 |
| 77210 | 1.77E-07 | 4.42E-08 | 1.41E-09 | 0.7953 | 0.1983 | 0.0063 |
| 88240 | 1.89E-07 | 4.71E-08 | 1.47E-09 | 0.7952 | 0.1986 | 0.0062 |
| 99270 | 2.00E-07 | 5.01E-08 | 1.52E-09 | 0.7951 | 0.1989 | 0.0060 |
| 110300 | 2.12E-07 | 5.31E-08 | 1.58E-09 | 0.7950 | 0.1991 | 0.0059 |

D.5. Low Peroxide Concentration Data

| | Effluent Moles | | | Effluent Mole % | | |
|---|---|---|---|---|---|---|
| Peroxide Concentration (PPM) | DBT | DBTO | DBTO2 | DBT | DBTO | DBTO2 |
| 0.00 | 4.34E-08 | 8.15E-09 | 2.97E-08 | 0.5341 | 0.1004 | 0.3655 |
| 551.50 | 4.61E-08 | 9.13E-09 | 3.58E-08 | 0.5064 | 0.1002 | 0.3934 |
| 1103.00 | 4.89E-08 | 1.01E-08 | 4.2E-08 | 0.4841 | 0.1000 | 0.4159 |
| 1654.50 | 5.17E-08 | 1.11E-08 | 4.82E-08 | 0.4658 | 0.0999 | 0.4343 |
| 2206.00 | 5.44E-08 | 1.21E-08 | 5.43E-08 | 0.4505 | 0.0998 | 0.4497 |
| 2757.50 | 5.72E-08 | 1.3E-08 | 6.05E-08 | 0.4375 | 0.0997 | 0.4628 |
| 3309.00 | 5.99E-08 | 1.4E-08 | 6.66E-08 | 0.4263 | 0.0996 | 0.4741 |
| 3860.50 | 6.27E-08 | 1.5E-08 | 7.28E-08 | 0.4166 | 0.0995 | 0.4838 |

D.6. 2:1 Flow Rate Ratio Data

| | Effluent Moles | | | Effluent Mole % | | |
|---|---|---|---|---|---|---|
| Reactor Residence Time (minutes) | DBT | DBTO | DBTO2 | DBT | DBTO | DBTO2 |
| 3.527066667 | 4.15E-07 | 1.17E-07 | 2.18E-09 | 0.7773 | 0.2186 | 0.0041 |
| 1.763533333 | 3.95E-07 | 1.09E-07 | 2.15E-09 | 0.7800 | 0.2158 | 0.0043 |
| 1.175688889 | 3.75E-07 | 1.02E-07 | 2.12E-09 | 0.7830 | 0.2126 | 0.0044 |
| 0.881766667 | 3.55E-07 | 9.44E-08 | 2.09E-09 | 0.7863 | 0.2090 | 0.0046 |
| 0.705413333 | 3.35E-07 | 8.70E-08 | 2.07E-09 | 0.7901 | 0.2050 | 0.0049 |
| 0.587844444 | 3.15E-07 | 7.96E-08 | 2.04E-09 | 0.7944 | 0.2005 | 0.0051 |
| 0.503866667 | 2.96E-07 | 7.22E-08 | 2.01E-09 | 0.7993 | 0.1952 | 0.0054 |
| 0.440883333 | 2.76E-07 | 6.48E-08 | 1.98E-09 | 0.8051 | 0.1892 | 0.0058 |

D.7. 4:1 Flow Rate Ratio Data

| | Effluent Moles | | | Effluent Mole % | | |
|---|---|---|---|---|---|---|
| Reactor Residence Time (minutes) | DBT | DBTO | DBTO2 | DBT | DBTO | DBTO2 |
| 2.645 | 2.15E-07 | 5.27E-08 | 1.68E-09 | 0.7980 | 0.1958 | 0.0063 |
| 1.764 | 2.21E-07 | 5.36E-08 | 1.68E-09 | 0.8001 | 0.1938 | 0.0061 |
| 1.323 | 2.28E-07 | 5.45E-08 | 1.69E-09 | 0.8022 | 0.1919 | 0.0059 |
| 1.058 | 2.34E-07 | 5.54E-08 | 1.69E-09 | 0.8041 | 0.1901 | 0.0058 |
| 0.882 | 2.41E-07 | 5.63E-08 | 1.69E-09 | 0.8060 | 0.1884 | 0.0057 |
| 0.756 | 2.48E-07 | 5.72E-08 | 1.69E-09 | 0.8077 | 0.1868 | 0.0055 |
| 0.661 | 2.54E-07 | 5.81E-08 | 1.70E-09 | 0.8094 | 0.1852 | 0.0054 |
| 0.588 | 2.61E-07 | 5.90E-08 | 1.70E-09 | 0.8110 | 0.1837 | 0.0053 |

D.8. 8:1 Flow Rate Ratio Data

| | Effluent Moles | | | Effluent Mole % | | |
|---|---|---|---|---|---|---|
| Reactor Residence Time (minutes) | DBT | DBTO | DBTO2 | DBT | DBTO | DBTO2 |
| 2.939 | 1.65E-07 | 3.92E-08 | 1.35E-09 | 0.8032 | 0.1902 | 0.0065 |
| 1.470 | 1.58E-07 | 3.76E-08 | 1.27E-09 | 0.8029 | 0.1906 | 0.0065 |
| 0.980 | 1.51E-07 | 3.60E-08 | 1.20E-09 | 0.8026 | 0.1911 | 0.0064 |
| 0.735 | 1.44E-07 | 3.44E-08 | 1.12E-09 | 0.8022 | 0.1915 | 0.0063 |
| 0.588 | 1.37E-07 | 3.28E-08 | 1.05E-09 | 0.8018 | 0.1921 | 0.0061 |
| 0.490 | 1.30E-07 | 3.12E-08 | 9.75E-10 | 0.8013 | 0.1926 | 0.0060 |
| 0.420 | 1.23E-07 | 2.96E-08 | 9.00E-10 | 0.8008 | 0.1933 | 0.0059 |

D.9. Effluent Tube Length Data

| | Effluent Moles | | | Effluent Mole % | | |
|---|---|---|---|---|---|---|
| Effluent Tube Residence Time (minutes) | DBT | DBTO | DBTO2 | DBT | DBTO | DBTO2 |
| 4.054 | 2.89E-07 | 7.27E-08 | 2.21E-09 | 0.7941 | 0.1999 | 0.0061 |
| 3.648 | 2.77E-07 | 6.93E-08 | 2.13E-09 | 0.7950 | 0.1988 | 0.0061 |
| 3.243 | 2.65E-07 | 6.59E-08 | 2.05E-09 | 0.7961 | 0.1977 | 0.0061 |
| 2.838 | 2.53E-07 | 6.25E-08 | 1.97E-09 | 0.7973 | 0.1965 | 0.0062 |
| 2.432 | 2.42E-07 | 5.91E-08 | 1.88E-09 | 0.7986 | 0.1952 | 0.0062 |
| 2.027 | 2.30E-07 | 5.57E-08 | 1.80E-09 | 0.8000 | 0.1937 | 0.0063 |
| 1.621 | 2.18E-07 | 5.23E-08 | 1.72E-09 | 0.8016 | 0.1921 | 0.0063 |
| 1.419 | 2.12E-07 | 5.06E-08 | 1.68E-09 | 0.8025 | 0.1912 | 0.0063 |
| 1.216 | 2.06E-07 | 4.89E-08 | 1.63E-09 | 0.8034 | 0.1903 | 0.0064 |
| 0.811 | 1.94E-07 | 4.54E-08 | 1.55E-09 | 0.8054 | 0.1882 | 0.0064 |
| 0.608 | 1.89E-07 | 4.37E-08 | 1.51E-09 | 0.8065 | 0.1871 | 0.0065 |
| 0.405 | 1.83E-07 | 4.20E-08 | 1.47E-09 | 0.8077 | 0.1858 | 0.0065 |
| 0.203 | 1.77E-07 | 4.03E-08 | 1.43E-09 | 0.8089 | 0.1846 | 0.0065 |

D.10. Peroxide Degradation Data

| | Effluent Moles | | | Effluent Mole % | | |
|---|---|---|---|---|---|---|
| Reactor Residence Time (minutes) | DBT | DBTO | DBTO2 | DBT | DBTO | DBTO2 |
| 3.527 | 3.16E-07 | 1.00E-07 | 6.01E-09 | 0.7482 | 0.2375 | 0.0142 |
| 1.764 | 3.19E-07 | 9.49E-08 | 5.59E-09 | 0.7602 | 0.2264 | 0.0133 |
| 1.176 | 3.22E-07 | 8.61E-08 | 5.16E-09 | 0.7790 | 0.2085 | 0.0125 |
| 0.882 | 3.25E-07 | 8.43E-08 | 4.74E-09 | 0.7847 | 0.2038 | 0.0115 |
| 0.705 | 3.27E-07 | 7.90E-08 | 4.31E-09 | 0.7972 | 0.1923 | 0.0105 |
| 0.588 | 3.30E-07 | 7.36E-08 | 3.88E-09 | 0.8099 | 0.1805 | 0.0095 |
| 0.504 | 3.33E-07 | 6.83E-08 | 3.46E-09 | 0.8228 | 0.1687 | 0.0085 |
| 0.441 | 3.36E-07 | 6.30E-08 | 3.03E-09 | 0.8358 | 0.1566 | 0.0075 |